Fossil Geyserite and Testate Amoebae in Geothermal Spring Vent Pools: Paleoecology and Variable Preservation Quality in Jurassic Sinter of Patagonia (Deseado Massif, Argentina)

Ana Julia Sagasti, Kathleen A. Campbell, Juan L. García Massini, Amanda Galar, Diego M. Guido, Pascale Gautret

Geobiology

WILEY

gebiology

ORIGINAL ARTICLE OPEN ACCESS

Fossil Geyserite and Testate Amoebae in Geothermal Spring Vent Pools: Paleoecology and Variable Preservation Quality in Jurassic Sinter of Patagonia (Deseado Massif, Argentina)

Ana Julia Sagasti[1,2] | Kathleen A. Campbell[3] | Juan L. García Massini[4] | Amanda Galar[2] | Diego M. Guido[2] | Pascale Gautret[5]

[1]School of Biological Sciences, Institute of Molecular Plant Sciences, The University of Edinburgh, Edinburgh, UK | [2]CONICET and Facultad de Ciencias Naturales y Museo, Universidad Nacional de La Plata, Instituto de Recursos Minerales (UNLP-CICBA), La Plata, Argentina | [3]School of Environment and Te Ao Mārama–Centre for Fundamental Inquiry, Faculty of Science, The University of Auckland, Auckland, New Zealand | [4]Centro Regional de Investigaciones Científicas y Transferencia Tecnológica (CRILAR), Provincia de La Rioja, UNLaR, SEGEMAR, UNCa, CONICET, Anillaco, La Rioja, Entre Ríos, Argentina | [5]Université d'Orléans, CNRS/INSU, BRGM, Institut des Sciences de la Terre d'Orléans (ISTO), UMR 7327, Orléans, France

Correspondence: Ana Julia Sagasti (anajusagasti@gmail.com; anaju.sagasti@ed.ac.uk) | Kathleen A. Campbell (ka.campbell@auckland.ac.nz)

Received: 1 August 2023 | **Revised:** 10 July 2024 | **Accepted:** 3 September 2024

Funding: This work was supported by Royal Society Te Apārangi, LE STUDIUM Multidisciplinary Institute for Advanced Studies (Orléans, France), and Agencia Nacional de Promoción Científica y Tecnológica.

Keywords: geyserite | hot-springs | paleoecology | Patagonia | sinter | testate amoeba

ABSTRACT

Geyserite is a type of terrestrial siliceous hot spring deposit (sinter) formed subaerially in proximal vent areas, with near-neutral pH, alkali chloride discharge fluids characterized by initial high temperatures (~73°C to up to 100°C) that fluctuate rapidly in relation to dynamic hydrology, seasonality, wind, and other environmental parameters. We analyzed sinters at the Claudia paleogeothermal field from the Late Jurassic (~150 Ma) Deseado Massif geological province, Argentinean Patagonia. The geyserite samples—with spicular to columnar to nodular morphologies—contain abundant microfossils in monotypic assemblages that occur in three diagenetic states of preservation. The best-preserved microfossils consist of vesicle-like structures with radial heteropolar symmetry (~35 μm average diameter), circular apertures, smooth walls lacking ornamentation, and disk- or beret-like shapes. Comparisons with extant, morphologically similar organisms suggest an affinity with the testate amoebae of the *Arcella hemisphaerica–Arcella rotundata* complex and *Centropyxis aculeata* strain *discoides*. These species occur in active geothermal pools between 22°C and 45°C, inconsistent with the temperature of formation of modern geyserites. We propose that the testate amoebae may have colonized the geyserite during cooler phases in between spring-vent eruptive cycles to prey on biofilms. Silica precipitation through intermittent bathing and splashing of fluctuating thermal fluid discharge could have led to their entrapment and fossilization. Petrographic analysis supports cyclicity in paleovent water eruptions and later diagenesis that transformed the opal into quartz. Spatially patchy degradation and modification of the silicified microorganisms resulted in variable preservation quality of the microfossils. This contribution illustrates the importance of microscale analysis to locate early silicification and identify high-quality preservation of fossil remains in siliceous hot spring deposits, which are important in early life studies on Earth and potentially Mars.

1 | Introduction

Geothermal systems typically occur in volcanically and tectonically active regions, where magmatic and convectively heated ground waters undergo water-rock interactions with the surrounding country rock to release solutes into the rising fluids (e.g., Jones and Renaut 2011; Sillitoe 2015; Jones 2021). Hot springs are the surface manifestations of geothermal systems that often contain high concentrations of dissolved silica (to ~500 ppm in spring vent fluids; Jones and Renaut 2011). The silica-rich thermal fluids emerge from depth to discharge from vents at variable intensities, frequencies, and temperatures (Munoz-Saez et al. 2023). Water temperatures range from ~25°C to a boiling point of 90°C–100°C, which can cool quickly depending on fluid discharge levels, water supply, wind, and seasonal climate (Renaut and Jones 2000; Jones and Renaut 2011; Munoz-Saez et al. 2023). As the waters cool and flow through discharge channels following the topography, evaporation and condensation lead to opaline silica precipitation in characteristic textures that may trap the local biota and reflect (micro)environmental conditions, particularly temperature, pH, water depth, and flow conditions (e.g., Henley and Ellis 1983; Hamilton, Campbell, and Guido 2019; Jones 2021 and references therein).

Geyserite is a type of siliceous hot spring deposit, or sinter, formed around proximal hot pools, geysers, and spouters as a result of the intermittent surging, splashing, and spraying of hot water (~73°C–100°C) from a nearby vent source (e.g., Braunstein and Lowe 2001; Lynne 2012; Campbell, Guido, et al. 2015; Campbell, Lynne, et al. 2015; Hamilton, Campbell, and Guido 2019; Munoz-Saez et al. 2023). In particular, the silica-rich, heated waters erupt from the vent source, with droplets falling onto and evaporating from surfaces of older sinter or bedrock, in a near-vent microenvironment known as the splash zone (Des Marais and Walter 2019). Upon cooling, precipitation and accumulation of finely laminated opaline silica occurs, producing geyserite—a dense, microbanded, ornate siliceous sinter deposit formed within a few meters of the spring-vent source (e.g., Braunstein and Lowe 2001; Lowe, Anderson, and Braunstein 2001; Lowe and Braunstein 2003; Lynne 2012; Campbell, Guido, et al. 2015; Campbell, Lynne, et al. 2015).

Microorganisms adapted to living in the splash zone of geysers include threads and biofilms of thermophilic archaea and bacteria that tolerate temperatures higher than 70°C (e.g., Castenholz 1969; Brock 1978, 1994; Jones and Renaut 1996; Meyer-Dombard, Schock, and Amend 2005; Meyer-Dombard et al. 2011). These thermophilic organisms act as templates for silica precipitation, whereby hot water droplets land on surfaces coated in extremophile biofilms and rapidly silicify and entomb the microbial encrustations in opaline silica (e.g., Cady and Farmer 1996; Jones and Renaut 2003; Handley et al. 2005; Campbell, Guido, et al. 2015; Campbell, Lynne, et al. 2015). Additionally, such biofilms have been shown to promote silica precipitation as nanospheres leading to the formation of Ediacara-style exceptional fossils (Slagter et al. 2022). The vertical accumulation of successive microbial biofilms and silica laminae results in stromatolitic build-ups in near-vent areas (e.g., Campbell, Guido, et al. 2015; Campbell, Lynne, et al. 2015; Guido et al. 2019). However, hot springs often display fluctuating environmental conditions that can lead to colonization by microorganisms adapted to moderate and cooler water temperatures when eruptive cycles wane and temperatures drop (e.g., Jones, Renaut, and Rosen 1997, 2003; Campbell, Guido, et al. 2015; Campbell, Lynne, et al. 2015, see their figure 1I, 46). Such mesophilic microorganisms can colonize vent areas during pauses in fluid flow and may prey on already-established biofilms (Jones, Renaut, and Rosen 2003). They then may become entrapped and silicified, although they are considered to be tenants of preexisting microbialites rather than active builders (Petryshyn et al. 2021).

Terrestrial hot spring deposits are of importance to paleontological and astrobiological research since they represent environmental conditions in which life may have originated on Earth and perhaps Mars (e.g., Konhauser et al. 2003; Guido et al. 2010; Campbell, Guido, et al. 2015; Campbell, Lynne, et al. 2015; Djokic et al. 2017; Westall et al. 2015, 2018; Cady et al. 2018). Most studies in modern hot spring systems rely on molecular methods to characterize microbial communities (e.g., Zhang et al. 2018; Meyer-Dombard, Schock, and Amend 2005; Meyer-Dombard et al. 2011; Sriaporn et al. 2020). Studies of fossil microbial communities, on the other hand, are based mainly on morphological analysis, which can limit the possibility of assigning taxonomic affinities. Nonetheless, morphology is a key feature that leads researchers to more detailed analytical and contextual investigations in geobiological studies (e.g., Farmer 1999; Van Kranendonk et al. 2019). However, morphology can become unreliable in investigating extremely ancient deposits (e.g., Archean), or those that have undergone advanced diagenesis, where nonbiologic objects of mineral or carbonaceous composition may be mistaken for microfossils or metabolic products of microorganisms (e.g., Schopf et al. 2005; Saitoh et al. 2021), or where biosignatures become degraded and obscured. Advanced analytic techniques (e.g., Raman spectroscopy, confocal laser spectroscopy, SIMS, etc.) have aided in the characterization of different structures and microscopic fossils, providing complementary information to morphological analyses (e.g., Kudryavtsev et al. 2001; Schopf and Kudryavtsev 2009; Marshall et al. 2012; Strullu-Derrien et al. 2019; Gangidine et al. 2021; Murphy et al. 2021). Trace element and REE geochemistry can also help determine the biogenicity of potential microbialites by detecting bioactive trace elements sequestered and preserved in microbialites (Webb and Kamber 2011; Gangidine et al. 2021; Nersezova et al. 2024). Thus, to better understand the constraints on the quality of fossil preservation in the geological record, the application of a combination of different techniques is pivotal to understanding the nature of putative microfossils, as well as the processes that affected both fossil formation and later impacts of diagenesis.

In this contribution, we present the first evidence of *bona fide* microfossils in Loma Alta geyserite samples of the Late Jurassic (~150 Ma) Claudia paleogeothermal field, Deseado Massif geological province, Argentine Patagonia. The geyserite preserves abundant microfossils constituting vesicle-like microorganisms with simple circular apertures and no ornamentation. We compare Claudia samples with microorganisms found in modern and fossil habitats of water-saturated geothermal microenvironments (e.g., Jones, Renaut, and Rosen 2003; García Massini et al. 2012, 2016; Benny, Humber, and Voigt 2014; Fernández, Lara, and Mitchell 2015; Strullu-Derrien et al. 2015, 2016; Sagasti

et al. 2019). The microfossils mostly resemble testate amoebae, unicellular amoeboid protists protected by a test (shell). The shape, ornamentation, and composition of these tests are species-characteristic and are used in morphology-based taxonomy (Tsyganov, Babeshko, and Mazei 2016; Anderson 2017; Marcisz et al. 2020). Herein, we examine the potential taxonomic affinities and environmental significance of the microfossils, as well as the effects of diagenesis on fossil preservation in a proximal vent paleogeothermal setting.

2 | Geological Background

2.1 | Deseado Massif Geothermal System

The Deseado Massif geological province in Patagonia, Argentina (Figure 1a) is a 60,000 km^2 region characterized by an extensive volcanic event of mafic and felsic magmatism caused by extension related to the opening of the South Atlantic Ocean in a diffuse back-arc tectonic setting during the Middle-Late Jurassic (~184.66–157.4 ± 0.65 Ma; Pankhurst et al. 2000; Riley et al. 2001; Richardson and Underhill 2002; Ruiz González et al. 2022). The volcanic and volcano-sedimentary rocks of the resulting Bahia Laura Volcanic Complex (Echeveste et al. 2001; Guido 2004) include: (1) andesites (Bajo Pobre Formation); (2) calc-alkaline rhyolite, minor andesite, rare dacite, extensive ignimbrites, and tuff layers (Chon Aike Formation); and (3) reworked volcaniclastic sediments in fluviolacustrine settings (La Matilde Formation) (Schalamuk et al. 1997; Marchionni et al. 1999; Echeveste et al. 2001; Guido and Campbell 2009; Guido et al. 2010). The volcanism was accompanied by extensive hydrothermal activity, resulting in low-sulfidation epithermal, precious metal mineralization, including several gold and silver deposits, and at least 23 ancient hot spring occurrences (Schalamuk et al. 1997; Guido and Campbell 2011).

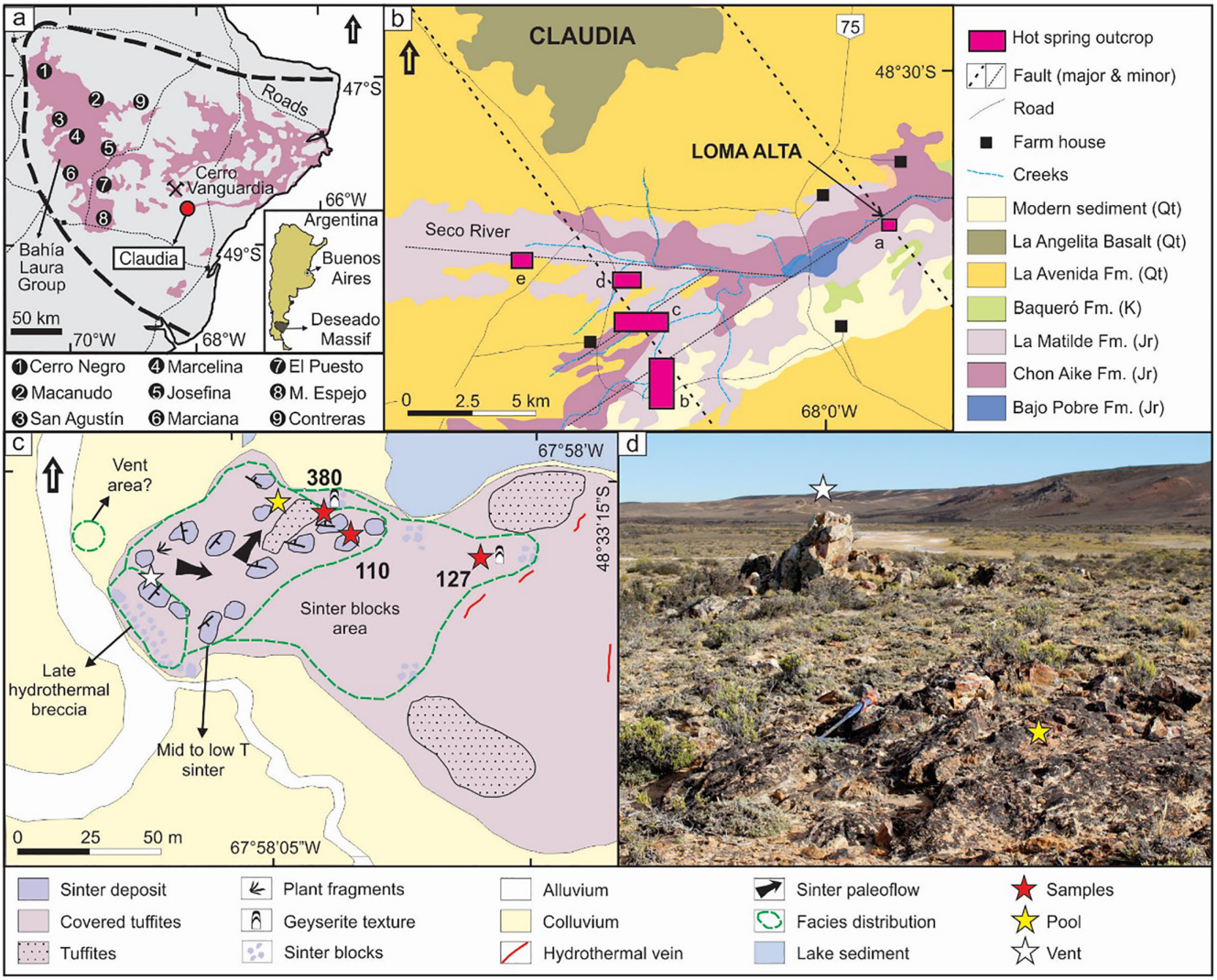

FIGURE 1 | (a) Map of the Bahía Laura Complex outcrops in the Deseado Massif. Numbers correspond to fossil hot-spring localities. Red circle marks Claudia locality. (b) Regional geological overview (from Guido and Campbell 2014) (a = Loma Alta, b = La Calandria Sur, c = La Calandria Norte, d = Lote 8 Este, e = Lote 8). (c) Geological map showing the distribution of hot spring deposits, facies, vents, and paleoflow (from Guido and Campbell 2014), with the addition of an interpreted vent (white star) and boiling pool (yellow star), and sampled sites (red stars). (d) View of the Loma Alta deposit and aligned vent (white star) and boiling pool (yellow star).

2.2 | Claudia Hot Spring Locality

The Claudia hot spring locality (Figure 1a; Guido and Campbell 2011, 2014) is the largest (40 km^2) and most lithologically and texturally varied paleogeothermal field preserved in the Late Jurassic Deseado Massif volcanic province (Guido and Campbell 2014). Both siliceous sinter and travertine are present, and facies range from extensive apron terraces to high-temperature subaerial vent mounds (Figure 1b; Guido and Campbell 2014; Guido et al. 2019). Within the Claudia paleogeothermal field, the Loma Alta deposit preserves proximal facies recognized by the co-occurrence of syndepositional faults, hydrothermal breccia, and geyseritic sinter textures (Guido and Campbell 2014).

At Loma Alta (Figure 1c,d), the outcrop encompasses a 150 m × 50 m area, exposed in an E–W direction, in which three facies were recognized: high-temperature sinter, mid- to low-temperature sinter, and hydrothermal breccia (Guido and Campbell 2014), following the criteria of Walter (1976) and published models of sinter deposition (e.g., Cady and Farmer 1996; Guido and Campbell 2011). Breccia fabrics at Loma Alta are characterized by angular fragments of high- and mid-temperature sinter blocks within an iron-rich silica matrix. The recognition of sinter breccia fabrics is of relevance for the reconstruction of hydrologic regimes of hot spring systems, since they can be indicative of explosive hydrothermal events (Browne and Lawless 2001), and may serve as conduits for spring-fluid upflow and outflow (e.g., Hedenquist and Henley 1985). Outcrops containing mid- to low-temperature sinter fabrics at Loma Alta are dominated by massive to faintly laminated silica layers, slightly undulatory to wavy in morphology, which in places contain lenticular voids resulting from bubble production within photosynthesizing microbial mats and hot spring degassing (see figure 4D of Guido and Campbell 2014, and figure 3 of Guido et al. 2019). The high-temperature sinter at Loma Alta is recognizable by the occurrence of spicular to columnar to nodular, densely and finely laminated geyseritic fabrics, which are typical for this facies (Guido and Campbell 2014).

Geyserite texture from the Loma Alta locality includes identified kerogen-rich (i.e., complex, insoluble, fossilized organic material) laminae alternating with silica (now quartz) layers, which indicates the presence of biofilms (Guido et al. 2019). All Jurassic sinters characterized in the Deseado Massif have diagenetically matured from noncrystalline amorphous silica to microcrystalline quartz (Guido and Campbell 2011). Despite diagenesis, lipid biomarker analysis of the Loma Alta sinter, particularly homohopane ratios, indicates that some portions of the deposits are thermally immature, which has resulted in excellent preservation (i.e., forming lagerstätten) of organic matter in some of the Loma Alta sinter (Teece et al. 2022).

3 | Materials and Methods

Fieldwork at the Late Jurassic Claudia hot spring locality (Figure 1a,b) was conducted in 2008, 2019, and 2020. Sampling at the Loma Alta sinter outcrops focused on three localities featuring well-preserved proximal apron and vent facies (cf. Guido and Campbell 2014; Campbell, Guido, et al. 2015; Campbell, Lynne, et al. 2015; Guido et al. 2019). Localities 110 and 380 consist of *in situ* blocks that are spatially close to hydrothermal breccia source areas, whereas locality 127 preserves scattered *ex situ* blocks that have rolled downhill as a product of recent erosion and weathering (Figure 1c, red stars). Hydrothermal source areas are interpreted based on the presence of hydrothermal breccia, fault lineaments, and geometry of the outcrops (Figure 1c,d, white and yellow stars, see Guido and Campbell 2014 for further description).

Hand samples were slabbed and polished to illuminate sinter textures and then selected portions were cut into standard thin sections (2 × 4 cm long/wide, 30 μm thick). Thin sections were examined under plane- and cross-polarized light microscopy using an Olympus BX53-P petrographic microscope at the Instituto de Recursos Minerales (INREMI, UNLP-CICBA, Argentina). Photomicrographs were taken with an Olympus UC30 camera mounted on the microscope. Sinter textures were studied at the meso and microscale from hand samples and thin sections, respectively. Sinter morphologic elements of densely laminated geyserite textures were classified following the criteria described by Walter, Grotzinger, and Schopf (1992), Campbell, Guido, et al. (2015), and Hamilton, Campbell, and Guido (2019). Diagenetic stages were defined based on petrography, SEM, and EDS analysis, with classification parameters identified by examining the size and distribution of quartz crystals, and the relative quality of fossil preservation.

For the morphological description of microfossils, thin sections of samples from localities 110, 380, and 127 of the Loma Alta outcrops were studied with optical light microscopy at INREMI (see details above). For each thin section, a minimum of 50 measurements of the diameter and aperture size of individual microfossils were made using Olympus Stream Start software. Photographs were edited with Adobe Photoshop 2020 using the photo-stacking technique to increase the depth of field (Piper 2010; Kerp and Bomfleur 2011). Rock slabs and petrographic thin sections are permanently hosted in the collection of the Museo Padre Molina in Río Gallegos, Santa Cruz Province, Argentina, under accession numbers MPM-EOS-23602–MPM-EOS-23610.

Confocal laser scanning microscopy was conducted at the Advanced Microscopy Facility of Facultad de Ciencias Exactas (UNLP) with a Leica SP5 confocal microscope. Samples were observed with 63× and 100× oil objectives, using fluorescence-free immersion oil, and a 633 nm laser excitation line. Z-stacks were constructed with micrographs taken at 0.5 μm steps to obtain three-dimensional reconstructions of the microfossils. The height of microfossils was measured from the z-stacks, considering the distance from the aboral to the oral end in the equatorial view. Images were processed with Fiji software.

For SEM and EDS investigations, samples were analyzed at Servicio de Microscopía Electrónica y Microanálisis (SeMFi–LIMF) of Facultad de Ingeniería (UNLP, Argentina), and at the Institut des Sciences de la Terre d'Orléans (ISTO, Orléans, France). At SeMFi-LIMF, samples were fragmented to obtain fresh surfaces, which were then washed with alcohol solution at 90% to eliminate modern contaminants, mounted with

graphite tape, and coated with gold to enhance conductivity. Samples were then examined under an FEI ESEM Quanta 200 Scanning Electron Microscope with a tungsten filament, using 20.00 kV voltage, under high and low vacuum. Due to difficulties illuminating heterogeneities in the samples, principal and backscattered electron techniques were applied. Energy dispersive spectroscopy (EDS) was performed to compare the elemental composition of fossils and matrix. EDS analyses at SeMFi-LIMF were performed with an Oxford EDS—AztecOne model probe with a high-speed SDD detector, resolution at energies <133 eV (in Mn Ka). Elemental spectra were measured on recognized fossils, as well as the surrounding matrix, and expressed as atomic percentages. At ISTO, thin sections were analyzed by scanning electron microscopy (SEM) with a TM 3000 (Hitachi) operating at 15 kV accelerating voltage, coupled with an energy dispersive X-ray spectroscopy (EDS) Swift ED 3000 X-Stream module (Hitachi), without coating. SwiftED3000 provided standardless quantitative analyses, normalized to 100%. The AZtecEnergy Analyser Software was used to display and interpret X-ray data to provide accurate and reliable standardless analysis (Burgess et al. 2007). The acquisition time for EDS point analyses was 240 s. Results were expressed as atomic percentages.

4 | Results

4.1 | Petrography and Geochemistry

Studied Loma Alta geyserite samples consist of stacked horizons (up to five successions evident in Figure 2a) of dark gray or white colored, thin and dense laminations exhibiting columnar, spicular, nodular, and cumulate textures (cf. Walter, Grotzinger, and Schopf 1992; Campbell, Guido, et al. 2015, and Hamilton, Campbell, and Guido 2019). Vertical cross-section views (Figure 2a–e) show that the geyserite horizons were typically initiated as successive, laterally continuous laminae with a gently undulating wavy texture referred to as pseudocolumnar (*sensu* Walter, Grotzinger, and Schopf 1992). These dense, very thin, parallel wavy laminae transition upward to laterally connected stacked sinter (cumulate texture) or to distinct columns that are erect, parallel, 1 mm–1.5 cm in diameter, and show branching styles that are lateral, bifurcate, or multifurcate (Figure 2a–f). In places, elongated sinter needles, 0.5–1 mm in diameter and up to 3 cm long (i.e., spicules) may be present (Figure 2c–e, white arrows). In other parts of the samples, coalesced columnar branching features may be present (Figure 2a,d–e black arrows). A dark siliceous matrix, in places appearing grainy and/or stained orange, fills the spaces between columns (Figure 2b–e). Individual geyserite columns measure, on average, 15 mm in height by 4.5 mm in width (e.g., Figure 2a,b), with columnar horizons commonly stacking successively upon each other (Figure 2a–e). In some samples (e.g., Figure 2f), the columns are particularly densely packed and grow outward and upward in a radiating pattern, thereby exhibiting a macrobotryoidal appearance (*sensu* Campbell, Guido, et al. 2015 and Hamilton, Campbell, and Guido 2019). In plan view (Figure 2g), the tops of columns merge laterally upon one another in a nodular texture, with some irregular columns indicating a coalescing of branches.

Under the microscope, the dense geyserite laminations show intercalation of light and dark silica bands, 25–50 μm thick (Figure 3a,b), with some showing marked, rounded terminations (Figures 3 and 4a,b). Near the base of many columns, the laminae display a gently undulating, wavy texture (pseudocolumnar, *sensu* Walter, Grotzinger, and Schopf 1992; e.g., Figure 3a (lower portion), 3b,c).

Petrographic analysis shows that the studied Jurassic geyserite samples occur in three different diagenetic types. Type 1 geyserite (Figure 4) is largely composed of nano to microcrystalline quartz, with sharp contacts between columns and the surrounding silica matrix, and containing well-preserved microfossils (i.e., dark brown colored and with sharp, continuously circular boundaries; Figure 4c,d). In Type 1 geyserite, the boundaries between columnar geyseritic sinter and the surrounding matrix are defined by small quartz microcrystals (7–10 μm; Figure 4b, black arrows); whereas, quartz macrocrystals (70–100 μm) may be present in fractures and pore spaces between columns (Figure 4a,b, white arrows).

Type 2 geyserite (Figure 5) is largely composed of micro and mesocrystaline quartz. The larger size of the crystals, compared with Type 1 geyserite, imparts a more transparent appearance to these samples. Microcrystals (7–10 μm) are more abundant within the sinter laminae (Figure 5b, white arrows). Mesocrystals (30–50 μm) are also present within laminae (Figure 5b, black arrows) but are more abundant in the siliceous matrix between columns. Macrocrystals (70–100 μm) appear in fractures, and in pore spaces in the silica matrix (Figure 5a,b, red arrows). In the Type 2 geyserites, microfossils are less abundant and many appear rather faint and ring-like, as well as somewhat grainy with irregular boundaries (Figure 5c, arrows).

A third form of geyserite (Type 3, Figure 6) is defined by quartz mesocrystals (30–50 μm long) that are abundant within the geyserite columns (Figure 6b,c, black arrows), and macrocrystals (70–100 μm) in greater abundance in the siliceous matrix in between columns (Figure 6a–c, red arrows). In some areas, the larger quartz crystals blur the boundaries between the geyserite columns and the siliceous matrix (Figure 6c). In Type 3 geyserite, microfossils are mostly absent. Scarce, faint molds appear in some areas (Figure 6d, arrows).

SEM and EDS analyses further illustrate the differences among the Type 1 and 2 geyserites (Figure 7, Table S1). In Type 1 geyserite, the microfossils can be recognized as rounded siliceous bodies distinct from the siliceous matrix (Figure 7a). Type 2 geyserite shows fossils preserved as ring-like molds in which the morphology of the microfossils is not fully preserved (Figure 7b,c, arrows). In some areas of Type 2 geyserite, the presence of microfossils is only indicated by rounded to irregular depressions in the siliceous matrix (Figure 7d,e) that are similar in size to the well-preserved microfossils in Type 1 samples. Type 1 geyserite samples show clear differences in elemental compositions between microfossils and matrix (Table S1), with fossils having twice as much carbon as the matrix. In Type 2 geyserites, EDS analysis of some samples shows the presence

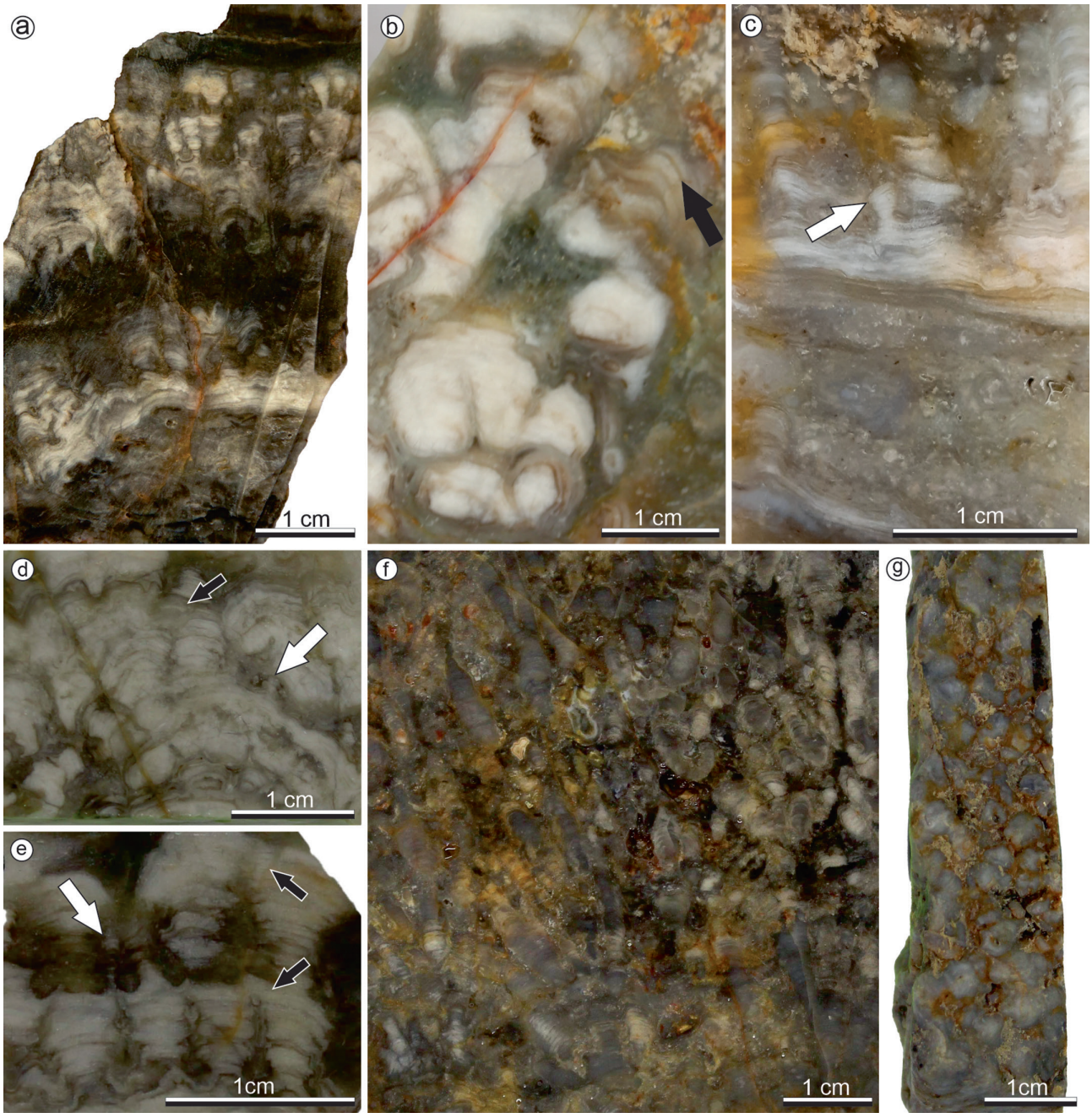

FIGURE 2 | Petrography of polished hand samples of studied Loma Alta geyserites. (a) Distinct, thin, and dense laminations of geyserite, up to five horizons visible in this sample, with each horizon initiating as laterally continuous pseudocolumns (*sensu* Walter, Grotzinger, and Schopf 1992) that then transition upward to cumulate texture or to various columnar branching styles (i.e., lateral, bifurcate, or multifurcate). Sample MPM-EOS-23603. (b) Detail of columnar geyserite texture comprising alternating laminae of relatively thicker white and very thin brownish gray (black arrow) silica. Dark gray, grainy, in places orange stained, siliceous sedimentary fill occupies spaces between geyserite columns. Sample MPM-EOS-23607. (c) Textural transition in a single, white geyserite horizon (upper half of image), from parallel wavy laminae (pseudocolumnar texture) at its base to erect, vertically parallel columns displaying varied branching styles (i.e., lateral, bifurcate). Lower portion of the image shows massive to faintly nodular laminated sinter, possibly nodular or macrobotryoidal geyserite. White arrow points to spicule. Sample MPM-EOS-23602. (d, e) Details of columnar geyserite, showing lateral coalescence (black arrows) as the columns grow upward, in places radiating in a divergent branching pattern seen in (d), with laterally linking bridges evident in (e) White arrows point to spicules. Samples MPM-EOS-23608 (d), MPM-EOS-23609 (e). (f) Radiating macro-botryoidal texture of densely packed geyserite columns. Sample MPM-EOS-23610. (g) Plan view of geyserite showing nodular to irregularly coalesced columns. Sample MPM-EOS-23606.

of Ti, a common detrital element in volcanic settings, and trace amounts of Cu, P, and As (Table S1). In addition, Type 2 geyserites show significantly higher concentrations of Al, Ca, and Fe (Table S1).

4.2 | Morphology of Microfossils

Samples, particularly of diagenetic Type 1 geyserites, show abundant, three-dimensionally preserved microfossils (Figure 8).

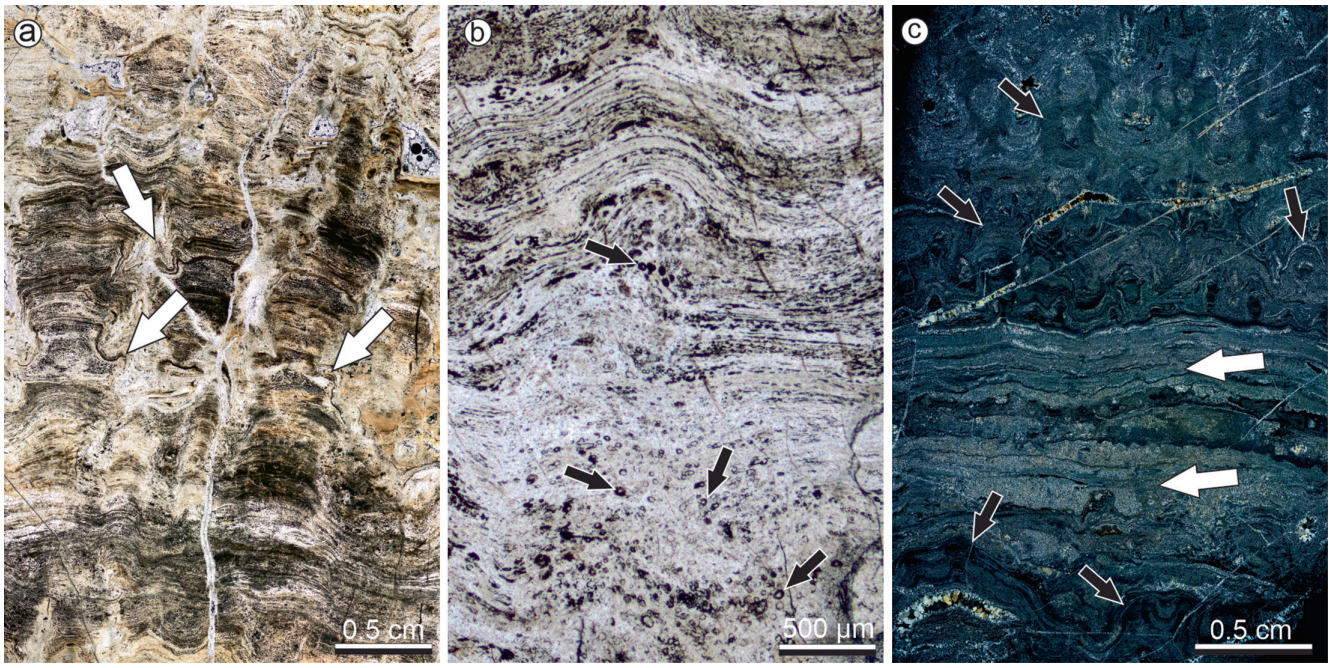

FIGURE 3 | Petrographic details of the studied geyserite sinter textures under plane- and cross-polarized light microscopy, ppl and xpl, respectively. (a) Petrographic thin section of geyserite texture showing intercalation of light and dark laminae stacked vertically in columns (> 5 mm wide), in places developing spicules (< 5 mm wide, white arrows). Sample: MPM-EOS-23603 a, ppl. (b) Detail of stacked lamination within geyserite pseudocolumn. Laminae are gently undulating and show alternating light and dark laminae. Microfossils appear in some laminae (dark circular features, some highlighted by black arrows). Sample MPM-EOS-23602 a-, ppl. (c) Alternation between columnar geyserite texture (black arrows, upper part of image) and wavy lamination (white arrows in lower part of the image). Sample MPM-EOS-23604 a, xpl.

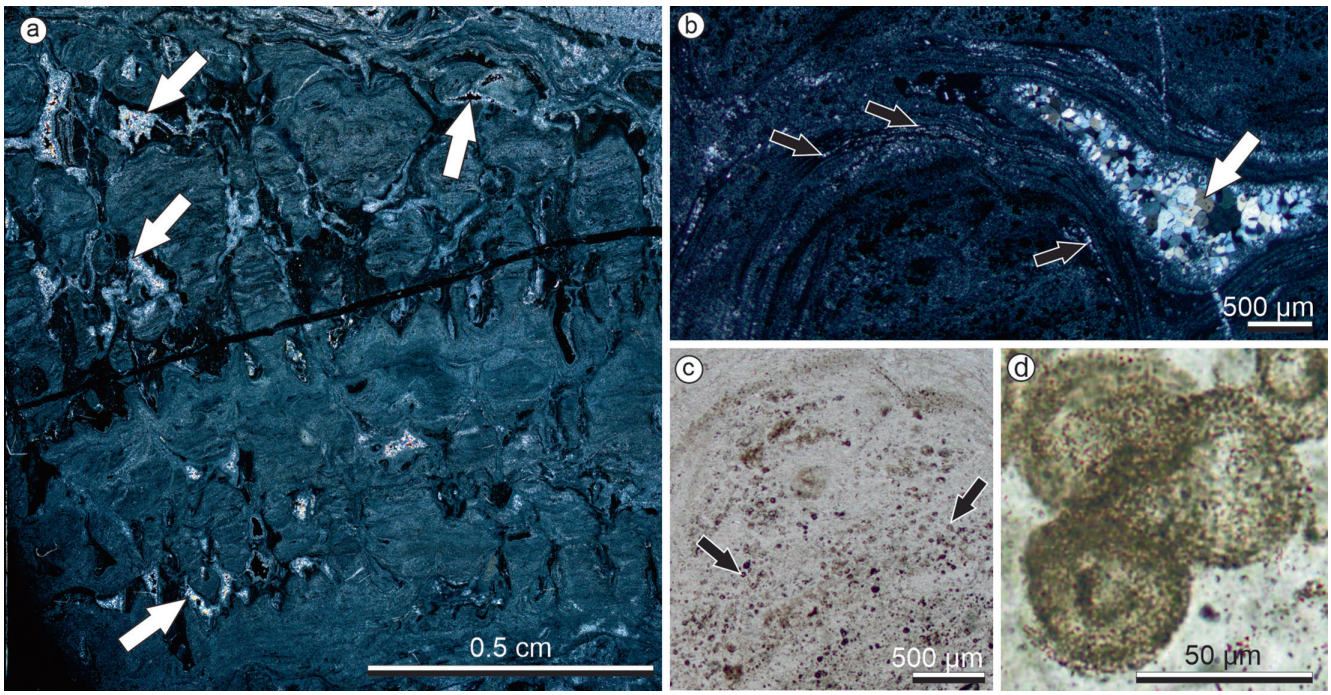

FIGURE 4 | (a) Type 1 geyserite showing columns (erect coalesced in lower part of the image, transitioning to erect bulbous and parallel to moderately divergent in upper part), largely composed of nano to microcrystalline quartz. White arrows point to voids and fractures between columns containing quartz macrocrystals. Sample MPM-EOS-23603 a, xpl. (b) Detail of lamination at the top of a rounded, single geyserite column. Microcrystals appear within laminae and at the outer boundary of the geyserite columns (black arrows). Macrocrystals occur in voids developed in the siliceous matrix (white arrow). Sample MPM-EOS-23608 a, xpl. (c) Well-preserved microfossils (some highlighted with black arrows) occurring within columns and spicules of Type 1 geyserite. Sample MPM-EOS-23608 a, ppl. (d) Close-up view of well-preserved microfossils, showing dark brown (organic-rich) color and distinctly circular and sharp outlines. Sample MPM-EOS-23608 a, ppl.

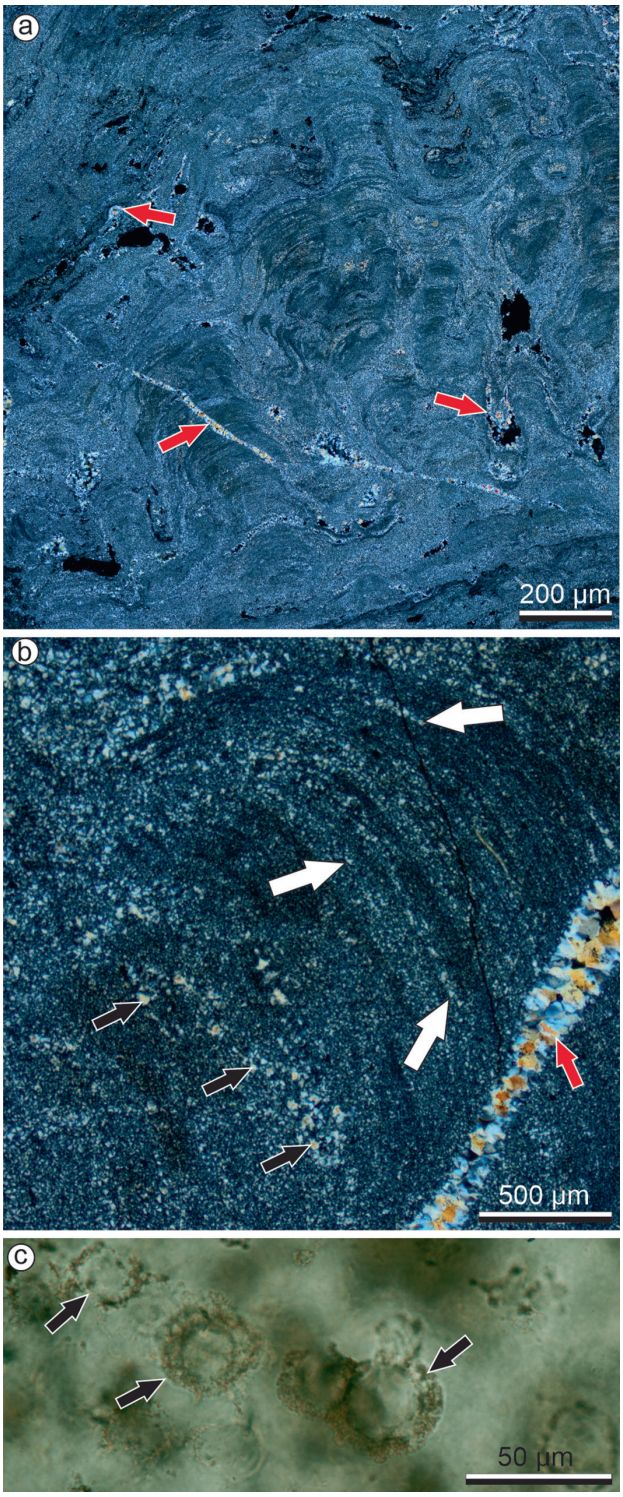

FIGURE 5 | Detailed petrography of Type 2 geyserites and microfossils. (a) Type 2 geyserite, largely composed of micro and mesocrystals of quartz. Macrocrystals cluster in voids in the siliceous matrix (red arrows) Sample MPM-EOS-23605 b, xpl. (b) Detail of a Type 2 geyserite column showing abundance of microcrystals aligned along lamination (white arrows) and mesocrystal concentrations (black arrows) within laminae. Macrocrystals appear in fractures (red arrow). Sample MPM-EOS-23605 b, xpl. (c) In Type 2 geyserites, microfossils are relatively light colored/translucent, and appear as faint rings (arrows) with less distinct boundaries compared to Type 1 geyserite microfossils. Sample MPM-EOS-23605 b, ppl.

The microfossils are circular in outline, with measured diameters of 12.14–64.49 µm (average = 35.24 µm) (Figure 8a–i). The aperture constitutes a simple circular opening at the oral pole, with a cross-section that ranges from 2.56 to 31.31 µm (average = 15.08 µm) (Figure 8b–e). The ratio between the total diameter and aperture diameter is 1.5–3.5. Fossil walls are smooth (Figure 8b–c,e,i), without appendages nor projections (Figure 8). An analysis with confocal laser scanning microscopy showed that samples emit autofluorescence between 647 and 738 nm when excited with the 633 nm laser (Figure 8e–i). The microfossils have radial heteropolar symmetry, with the axis of symmetry extending from the center of the oral pole to the center of the opposite, aboral end (Figure 8f,h,i). In equatorial view, the microfossils are discoid to hemispherical and have heights of 9.87–19.3 µm (Figure 8f,h). The height-diameter ratio ranges between 0.2 and 0.3 (Figure 8f,h,i).

5 | Discussion

5.1 | Paleohydrological Regime

The analysis of microtextures and fabrics preserved in sinter deposits can aid in the interpretation of the paleohydrological regime (e.g., Braunstein and Lowe 2001), as well as recognition of early to postdepositional diagenetic pathways preserved in a fossil hot spring deposit (e.g., Campbell et al. 2001, 2019; Lynne et al. 2007; Guido and Campbell 2011). Textures observed at the Loma Alta locality in the Claudia paleogeothermal field consist of columns of geyserite laminae, which show various branching styles (Figures 2–6) and coalesce laterally and stack vertically upon one another, and in places develop narrow spicules.

Spicular to columnar geyserite textures are a common feature in Miocene to Recent hot spring systems from the Taupo and Coromandel volcanic zones (New Zealand), and in modern geothermal fields of Yellowstone National Park (U.S.A.) and El Tatio (Chile) (Table 1; e.g., Braunstein and Lowe 2001; Jones and Renaut 2006; Campbell, Guido, et al. 2015 and references therein, Jones 2021; Murphy et al. 2021; Munoz-Saez et al. 2023). In Yellowstone National Park (Y.N.P.) and at El Tatio, geyserite structures forming at the rims of boiling pools are thinner (i.e., spicular) closer to the vent, and wider (columnar, nodular) farther away from the vent (Braunstein and Lowe 2001; Munoz-Saez et al. 2023). This morphological gradient can also be observed at Y.N.P. spring-vent pools, where spicules (< 1 mm wide) develop on poolward (inner) rims as the product of direct splash or waves; whereas, wider columns (1–3 cm) occur in the outer rims farther away from the direct splash area of the vent, at temperatures ranging between 40°C and 65°C (Cady and Farmer 1996; Braunstein and Lowe 2001). Based on textural features, we infer that the geyserites from the Claudia paleogeothermal field were formed around the outer rims of hot pools under intermittent splashing and surging conditions. Localities 110 and 380 are both proximal to the interpreted source point (Figure 1c, red and yellow stars). Samples from locality 127 originate from *ex-situ* blocks; hence, their relationship with the source point cannot be established.

Sharp contacts between geyserite columns/spicules and the surrounding siliceous matrix (e.g., Figure 2b–e) indicate

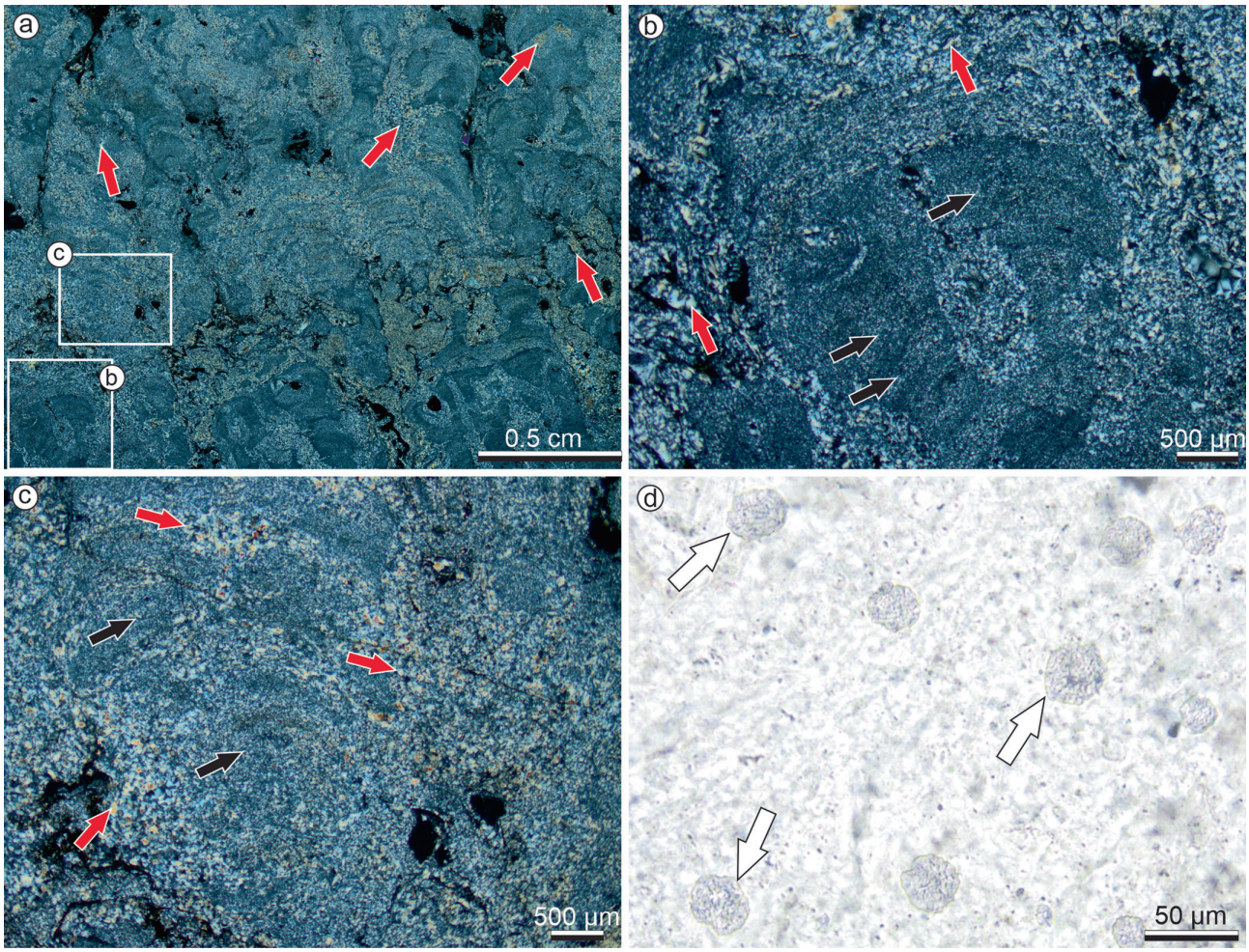

FIGURE 6 | (a) Advanced crystallization of Type 3 geyserite columns, with red arrows indicating quartz macrocrystals. Sample MPM-EOS-23606 c, xpl. (b–e) Detail of two areas of Type 3 geyserite. Micro and mesocrystals are abundant, both in between laminae and in the siliceous matrix. Black arrows point to mesocrystals between the laminae. Macrocrystals are abundant in the siliceous matrix (red arrows). In (b) the limits between the stacked sinter and siliceous matrix are still visible, whereas in (c) these limits are blurred by the size increase of quartz crystals. (d) Occurrences of faint microfossils (white arrows). Sample MPM-EOS-23606 c, ppl.

hiatuses in silica precipitation, either during episodic pulses in vent fluid discharge or over relatively long spells of geyser inactivity (cf. Braunstein and Lowe 2001). The alternating white and gray sinter laminae, and branching/radiating upward growth of many geyserite columns (Figure 2), mark recurring starting and stopping of the growth of these features in the Claudia sinter. Moreover, these alternations in dark and light laminae in the Claudia geyserite (Figures 2 and 3) may be indicative of rapid versus slow evaporation/precipitation, respectively (Jones and Renaut 2004; Campbell, Guido, et al. 2015). Jones and Renaut (2004) found that dark laminae are initially deposited as a hydrous silica gel, or "wet opal"; whereas, light laminae comprise "dry opal" formed by evaporation/desiccation of thin films of wet opal, following the eruptive cyclicity of the system.

5.2 | Diagenetic Pathways

In this study, geyserite diagenetic Types 1–3 illustrate both the primary cyclicity of vent activity and initial silicification, as well as a progression of later (postdepositional) diagenesis affecting the quality of microfossil preservation. Samples from locality 380 all correspond with Type 1 geyserites; whereas, samples from locality 110 are more variable, showing both Type 1 and 2 geyserites, sometimes in the same hand sample. Type 3 geyserites were observed in samples from locality 127, and in small patches of some samples from locality 110.

The petrographic features observed in Type 1 geyserite are consistent with the highest quality of fossil preservation via early/rapid silicification during early diagenesis (Knoll 1985; Cady and Farmer 1996; Campbell et al. 2001; Maliva, Knoll, and Simonson 2005). Early and typically rapid silicification has long been touted as the driver for the formation of lagerstätten deposits in many terrestrial and marine hydrothermal settings in the geological record (e.g., Knoll 1985; Cady and Farmer 1996; Trewin 1993; Jones, Renaut, and Rosen 1997, 2001; Fayers and Trewin 2003; Jones and Renaut 2003; Maliva, Knoll, and Simonson 2005; Handley et al. 2008; Channing and Edwards 2009; Channing and Wujek 2010; Campbell, Guido, et al. 2015; Campbell, Lynne, et al. 2015; Westall et al. 2015).

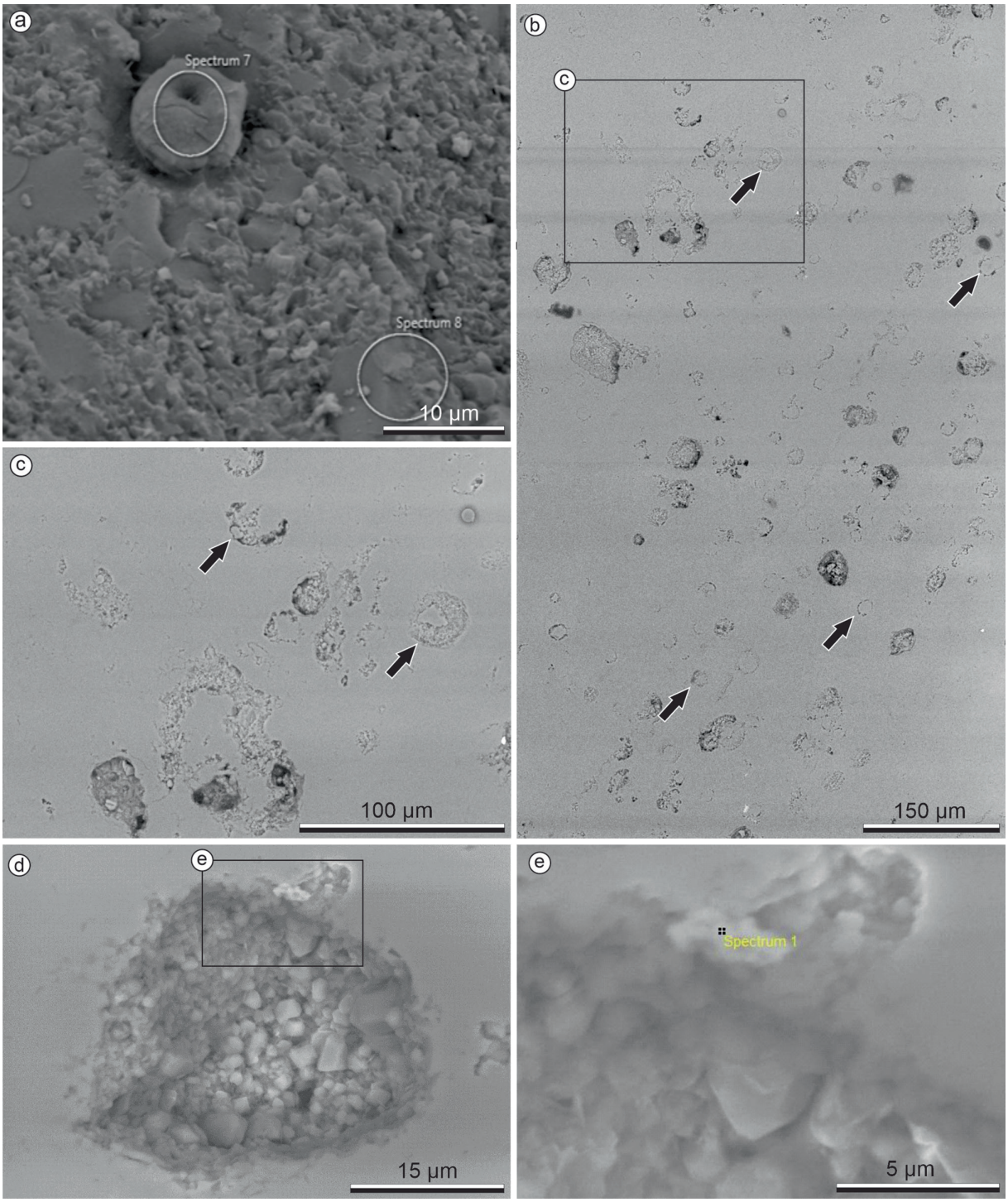

FIGURE 7 | SEM analysis of Type 1 (a, Sample MPM-EOS-23603) and 2 (b-e, Sample MPM-EOS-23607) geyserite. (a) SEM micrograph of Type 1 geyserite showing a microfossil (labeled with a circle and Spectrum 7). Points at Spectrum 7 and 8 mark the spots of EDS measurements (see Table S1). (b) Type 2 geyserite with ring-like molds of microfossils (arrows). (c) Detail of the microfossil molds in b, arrows. (d) Depression in the siliceous matrix marks places where a microfossil was preserved and later altered by diagenesis. (e) Close-up of depression edge with EDS spot (Spectrum 1) representative for type 2 geyserite (see Table S1).

Organic geochemistry analysis (vitrinite reflectance equivalent and homohopane ratios) of breccias associated with geyserite from locality 110 yields values indicative of their immaturity and exceptional preservation of the organic matter (Teece et al. 2022).

In Type 2 geyserite at Claudia, diagenetic quartz crystals occupy more spaces, displacing original biotic features. The microfossils are preserved as relatively fainter, ring-like features with less distinctive boundaries, indicating moderate diagenetic modification of the original life forms. Lastly owing to a more

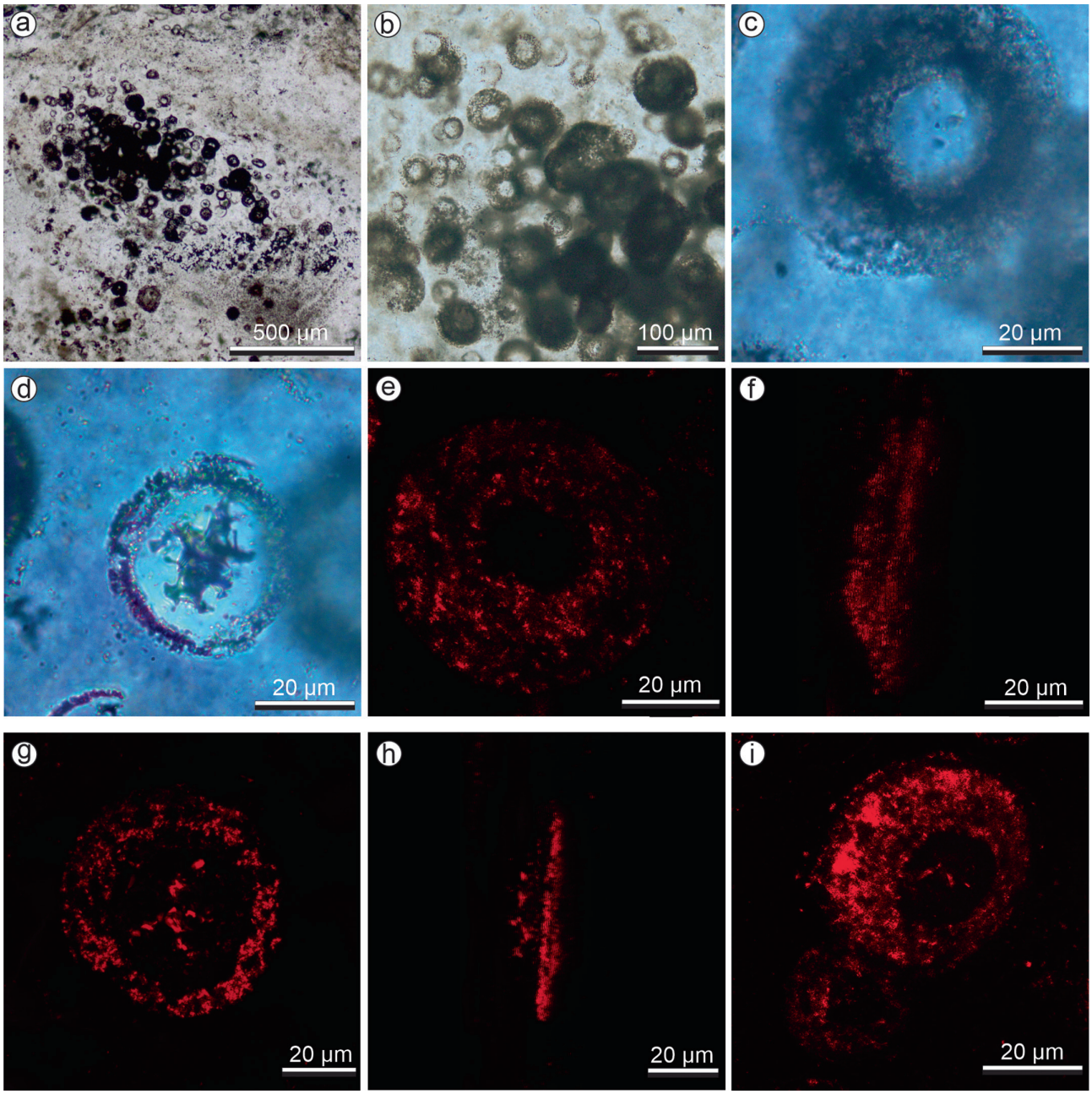

FIGURE 8 | Fossilized potential testate amoebae from the Loma Alta Type 1 geyserite at the Claudia paleogeothermal field. Sample MPM-EOS-23603 b (a) Microfossils aggregated in clusters within geyserite textures. (b) Group of microfossils showing discoid shapes and circular apertures. (c) Close-up of individual microfossil, potentially testate amoeba, showing circular aperture and relatively smooth test wall. (d) Detail of microfossil with quartz micro crystals partially filling the interior of the test. Test is preserved in a Type 1 geyserite but shows a locally more advanced stage of alteration of the original morphology. (e, f) Confocal laser microscopy of microfossils in polar (e, g, i) and equatorial (f, h) views.

complete secondary diagenesis, Type 3 geyserite contains the largest size of quartz crystals, merging of boundaries between the geyserite columns and matrix, and bears only a few quite faintly preserved microfossils.

In general, proximal apron and vent mound facies do not preserve well in the geological record because of their subaerial and localized nature, subjected to destruction and active weathering in dynamic volcanic and tectonic environments (Campbell, Guido, et al. 2015). Moreover, patchy diagenesis in Phanerozoic sinters is known to cause partial to complete obliteration of original sinter textures (e.g., Campbell et al. 2001, 2019; Jones 2021). During burial diagenesis, sinter deposits may become massive and original structures and textures such as lamination that are typically used for facies interpretations become obscured (e.g., Walter, Grotzinger, and Schopf 1992; Campbell et al. 2001). In this study, the patchy nature of diagenesis of the Jurassic sinter is evidenced in samples from locality 110 that show both Type 1 and 2 geyserites in the same hand sample.

TABLE 1 | Comparative table with geyserite textures described here (for Claudia locality) and in modern hot spring settings El Tatio, Chile (Munoz-Saez et al. 2023), Yellowstone National Park, U.S.A. (Braunstein and Lowe 2001), Taupo Volcanic Zone, New Zealand (Jones and Renaut 2006).

Textural features	Claudia locality	El Tatio		Yellowstone National Park	Taupo Volcanic Zone
Age	Late Jurassic	Modern		Modern	Modern
Texture	Nodular	Spicules	Columns	Columns	Spicules
Average height	15 mm	< 1 cm	Up to 2.5 cm	Up to 10 cm	< 3 cm
Average width	4.5 mm	< 5 mm	> 5 mm	1–3 cm	≤ 5 mm
Shape	Columns stacked upon each other. Base is narrower than apex. Columns may coalesce or present narrow crevices between one another	Cross-section mostly circular. Spicles tend to merge and branch upward. They may coalesce to form columns	Cross-section ellipsoidal to irregular. Usually independent columns separated by crevices	Circular to polygonal cross-section. Columns are separated by narrow crevices	Narrow upward-tapering structures with a rounded convex apex
Microenvironment within the hot spring	At the margins of boiling pools (inferred)	100% at 0.2 m from vent 75% spicules at 0.7 m from vent	75% columns at 1.2 m from vent	Rims of pools with subaqueous vents. The inner rims (poolward) develop spicules less than 1 mm in diameter, whilst the outer rim presents the columns	Along the margins of boiling pools, and on raised areas, aprons, and outflow channels around spring pools
Temperature (°C)	20–65 inferred	29.5–70.3	20–55.1	40–65	18–86

5.3 | Paleoecology and Taxonomic Affinities of Microfossils From Claudia

A variety of modern soil-dwelling and wetland microorganisms produce vesicle-like structures as part of their life cycles (Watkinson, Boddy, and Money 2016; Archibald, Simpson, and Slamovits 2017). Similar structures to those studied here can be found among the chytridiomycetes (chytrids), zygomycetes (pin molds), peronosporomycetes (water molds), and amoebae (Table S2). These groups of microorganisms have members that live or have been found fossilized in geothermally influenced environments (e.g., Jones, Renaut, and Rosen 2003; García Massini et al. 2012, 2016; Benny, Humber, and Voigt 2014; Fernández, Lara, and Mitchell 2015; Strullu-Derrien et al. 2015, 2016; Sagasti et al. 2019). The simple morphology, vesicle shape, and circular aperture of the microfossils resemble chytrid sporangia (Powell and Letcher 2014), asexual phases of zygomycetous fungi such as sporangia and conidia (Benjamin 1979; Benny, Humber, and Voigt 2014), and peronosporomycetes oogonia (Dick 2001). However, both chytrids and zygomycetes live as parasites or saprotrophs (e.g., Powell 1993; Benny, Humner, and Morton 2001; Benny, Humber, and Voigt 2014; Powell and Letcher 2014), whilst peronosporomycetes oogonia are variably ornamented with appendages or wall projections (Dick 2001). The microfossils studied here do not appear to be associated with plant or animal remains, nor do they present ornamentation appendages; therefore, they most likely have a different origin.

The thermophilic amoeba *Naegleria fowleri* inhabits modern hot springs and produces vesicular cysts as part of their life cycle (Barnhart et al. 2024). *N. fowleri* has been found in geothermal waters with temperatures ranging between 18.6°C and 46.4°C in the Grand Teton National Park (Wyoming, U.S.A.; Barnhart et al. 2024). The cysts of *Naegleria* are vesicle-like structures with a very thick fibrous wall with ostioles (small, pore-like apertures) (Evdokiou, Marciano-Cabral, and Jamerson 2021). The size of these cysts ($\leq 10\,\mu m$) and the lack of a circular aperture differentiate them from the microfossils found at Claudia.

Testate amoebae form diverse and abundant communities in freshwater and terrestrial habitats, including soils, bogs, wetlands, sewage treatment waters, and hot springs (e.g., Ellison and Ogden 1987; Charman et al. 2000; Beyens and Meisterfeld 2002; Jones, Renaut, and Rosen 2003; Mazei and Tsyganov 2006; Fernández, Lara, and Mitchell 2015; Tsyganov, Babeshko, and Mazei 2016; Marcisz et al. 2020). The most common testate amoebozoans in modern hot spring systems are *Arcella, Centropyxis, Trinema, Difflugia*, and *Euglypha* (Table 2; e.g., Ehrenberg 1843; Jung 1942; Dogiel 1965; Winterbourn and Brown 1967; Jones, Renaut, and Rosen 2003; Fernández, Lara, and Mitchell 2015). These testate amoebae can be found in different subenvironments within geothermal systems, particularly in low- to moderate-temperature settings such as pools, aprons, outflow channels, and geothermally influenced wetlands. The genera *Centropyxis, Trinema*, and *Difflugia* are found in waters at 40°C–45°C (Dogiel 1965). Species of *Arcella, Difflugia*, and *Euglypha* have been recorded in hot springs from the Taupo Volcanic Zone (New Zealand) at temperatures of 22°C, 45.3°C, and 24.5°C, respectively (Winterbourn and Brown 1967). *Euglypha* also has been recorded on the flanks of a geyser mound, where waters had cooled from ~80°C to 41°C (Jones, Renaut, and Rosen 2003). *Arcella rotundata*, *Centropyxis aculeata, C. cassis, Euglypha leavis*, and *Trinema enchelys* have been reported in moderate-temperature hot springs of Chile (Ehrenberg 1843; Jung 1942; Fernández, Lara, and Mitchell 2015). Of these genera, the most morphologically similar to microfossils from Claudia are *Arcella* and *Centropyxis* (Table 3). *Centropyxis cassis* has ovoid agglutinated tests with a thick organic lip in the aperture (Siemensma 2023) that clearly differentiate it from the microfossils. *Centropyxis aculeata* strain *discoides* (*Centropyxis discoides sensu* Ogden and Hedley 1980; their Plate 16, 54) has a smooth-walled proteinaceous test and discoid shape (Ogden and Hedley 1980). However, the dimensions of this species are much larger than the Claudia microfossils (150–300 μm in diameter, 50–100 μm aperture diameter, 38–75 μm height). When considering the proportions of the test, *Centropyxis discoides* resembles the fossils described here, with a total diameter-to-aperture ratio of 3–3.5 and a height-to-diameter ratio of 0.25–0.3. Testate amoeba of the *Arcella hemisphaerica–Arcella rotundata* complex (Lahr and Lopes 2009) have tests that are circular in oral view and hemispherical in equatorial view. The tests are chitinous and are built up from hollow hexagonal units with small pores (1–2 μm) at each vertex of the hexagons (Lahr and Lopes 2009). Tests are 55–65 μm in diameter, 25–35 μm height, with an aperture of 15–25 μm

TABLE 2 | Morphological characteristics and range of temperatures known for modern testate amoebae living in hot springs.

Taxon	Shape	Temperature in hot springs
Difflugia ssp.	Agglutinate test with terminal aperture that is round, oval, lobed, or toothed, sometimes with a collar	40–45
Centropyxis ssp.	Discoid to beret tests, proteinaceous or agglutinant. Aperture circular to uneven, always central	40–45
Trinema	Test composed of scales. Aperture subterminal, ventral, circular to oval, surrounded with toothed plates	40–45
Euglypha	Test elongate ovoid or pyriform, composed of overlapping plates. Aperture always ornamented	41–80
Arcella	Organic test, more or less circular, with central invaginated aperture	22
Microfossils	Organic discoid to hemispheric test. Central circular aperture	40–65

TABLE 3 | Comparison of the main sizes and ratios of measured tests of microfossils from Claudia, the modern *Arcella hemisphaerica–Arcella rotundata* complex, and the modern *Centropyxis aculeata* strain *discoides*.

Taxon	Test diameter	Aperture diameter	Diameter/Aperture ratio	Height	Height/Diameter ratio	Temperature in hot springs
Claudia microfossils	12.14–64.49 (x = 35.24)	2.56–31.31 (x = 15.08)	1.5–3.5	9.87–19.3	0.2–0.3	20–65 inferred
Arcella hemisphaerica-Arcella rotundata complex	55–65	15–25	2.6–3.6	25–35	0.25–0.75	22
Centropyxis aculeata strain *discoides*	150–300	50–100	3–3.5	38–75	0.25–0.3	40–45

in diameter. The test height/diameter ratio for *Arcella hemisphaerica-–Arcella rotundata* complex is 0.25–0.75 (average 0.51). The general shape, dimensions, and proportions of the tests of the *Arcella hemisphaerica—Arcella rotundata* complex are quite similar to microfossils from Claudia. The main difference is the absence of hexagonal units with small pores in the microfossils from Claudia. However, this fine detail of the test could have been lost because of diagenesis. The specific affinities of the studied samples are not straightforward to assess, since only broad morphological characters of the tests are preserved, but both *Arcella rotundata* and *Centropyxis aculeata* have been found in modern hot springs from Chile, which could indicate the affinity of the Argentine microfossils.

In recent years, protozoologists have suggested that the shape and size of tests of amoebae are not a reliable character to assign systematic affinities, owing to a tendency toward morphological convergence of genera that live in similar environments (e.g., Schulz et al. 2018; McKeown et al. 2019; González-Miguéns et al. 2022). Nonetheless, the use of functional traits of testate amoebae has been established as indicators of environmental parameters (Lamentowicz et al. 2020; Marcisz et al. 2020; Šímová et al. 2022). Amoebae with tests that are compressed, subspherical, discoidal, or hemispherical are adapted to living in thin water films (Marcisz et al. 2020). Additionally, a beret-like morphology (i.e., circular outline, compressed test, central aperture) is associated with stressed conditions such as low pH or the presence of contaminants such as metals (Marcisz et al. 2020). Fluctuation of the water table in the Claudia hot springs is evident by sedimentary structures such as the intercalation of columnar and thinly laminated sinter that we interpret to result from alternating wet-dry conditions. In addition, EDS analysis of Type 1 and 2 geyserite shows the presence of Al, Ca, and Fe in both types, and P, Ti, Cu, and As in Type 2 (Table S1). However, high concentrations of precious- and base metal elements have been related to postdepositional detrital influx rather than initial formation concentrations of sinters (Sillitoe 2015) which is more consistent with a diagenetic origin for the metals seen in Type 2 geyserite. The patchy distribution of Types 1–3 geyserite makes it difficult to conduct systematic investigations of the elemental composition of many samples to fully rule out the presence of metals as influxes at the time of sinter precipitation.

Geothermal systems are dynamic and unstable in their environmental conditions. In particular, the vent proximal zone is characterized by oscillations between eruptions of hot water and cooler intervals of inactivity for a given geothermal system (Jones, Renaut, and Rosen 2003). This typically nonperiodic cyclicity allows for biota that usually inhabits cooler waters to thrive for a time in proximal vent deposits not inundated constantly by boiling waters (Jones, Renaut, and Rosen 2003). During eruptive periods, when water temperatures can reach up to 90°C, only thermophile microbial biofilms can establish themselves and flourish at the rims of boiling pools. The presence of kerogen laminae identified with Raman mapping (Guido et al. 2019) in Loma Alta geyserite is indicative of the establishment of such microbial biofilms. Testate amoebae at Claudia could have colonized similar microbial substrates to feed during the cooler phases between vent eruptions and perhaps took refuge in distal areas of the outflow once the rising temperature cycle resumed.

6 | Conclusions and Future Directions

Samples studied at the Late Jurassic Loma Alta hot spring locality at the Claudia paleogeothermal field in Argentinean Patagonia show geyserite sinter textures and contain vesicles inferred as microfossils.

The microfossils studied herein are interpreted as testate amoebae. The morphology and proportions of the tests suggest an affinity with the extant *Arcella hemisphaerica—Arcella rotundata* complex and *Centropyxis aculeata* strain *discoides*, both known from modern hot spring systems. Testate amoebae in terrestrial hot springs occur in waters of 40°C–45°C; whereas, geyserite forms in near-vent areas where waters erupt at >70°C. However, the cooling patterns and intermittency of the eruptions can promote microenvironmental conditions compatible with the presence of testate amoeba. Additionally, the presence of thermophilic biofilms in the splash zone could provide a food source for the testate amoeba to graze on. Once the eruptive cycle is resumed, silica precipitation at the margins of this boiling pool would have led to the fossilization of these amoebae.

The geyserite is preserved in three diagenetic stages differentiated firstly by the increase in the size of the quartz crystals as diagenesis progressed from early to late, with a transition from predominantly nanocrystalline to mesocrystalline with an accompanying increase of macrocrystals. The increase in quartz crystal size coincides with the preservation state of the observed microfossils. Areas predominantly composed of nanocrystalline quartz contain well and fully preserved microfossils with intact carbon-rich shells, whereas areas with abundant meso and macrocrystals only preserve irregularly circular ring-like features to near absent fossils. The diagenetic stages show a patchy distribution within hand samples that can contain more than one diagenetic type. Hence, this diagenetic progression illustrates the difficulties that may be encountered in the study of ancient hot spring systems, the importance of understanding processes of fossilization and biosignature degradation, as well as the impact of diagenesis on fossil quality, and thus should be taken into consideration when studying early life on Earth and possibly elsewhere in the Solar System.

Acknowledgments

We thank the Culture Bureau of Santa Cruz Province for supporting our research and granting us the research permits to study the Bahía Laura Complex deposits in the Deseado Massif. We thank four anonymous reviewers and the Editors from Geobiology for their comments that helped to improve our manuscript significantly. Funding for this project was provided by PICT 2020-SERIE A-02000 (to Ana J. Sagasti), a Senior Scientist Fellow award to Kathleen A. Campbell (K.A.C.) from the LE STUDIUM Multidisciplinary Institute for Advanced Studies (Orléans, France), and the Royal Society of New Zealand Te Apārangi Marsden Fund (to K.A.C.). We thank Dr. Anna Šímová for fruitful discussions on the ecology and population dynamics of extant centropyxids, and Dr. Leonardo Fernández for information about testate amoebae in Chilean hot springs.

Conflicts of Interest

The authors declare no conflicts of interest.

Data Availability Statement

Data are available from the corresponding author (A.J.S.) upon reasonable request.

References

Anderson, O. R. 2017. "Amoebozoan Lobose Amoebae (Tubulinea, Flabellinea, and Others)." In *Handbook of the Protists*, edited by J. M. Archibald, A. G. B. Simpson, and C. H. Slamovits, 1279–1309. Cham: Springer. https://doi.org/10.1007/978-3-319-32669-6_2-1.

Archibald, J. M., A. G. B. Simpson, and C. H. Slamovits. 2017. *Handbook of the Protists*. Second ed, 1662. Cham: Springer.

Barnhart, E. P., S. M. Kinsey, P. R. Wright, et al. 2024. "*Naegleria fowleri* Detected in Grand Teton National Park Hot Springs." *ACS ES&T Water* 4, no. 2: 628–637. https://doi.org/10.1021/acsestwater.3c00650.

Benjamin, R. K. 1979. "Zygomycetes and Their Spores." In *The Whole Fungus*, edited by B. Kendrick, 573–616. Ottawa: National Museum of Natural Sciences and the Kanaskis Foundation.

Benny, G. L., R. A. Humner, and J. B. Morton. 2001. "Zygomycota: Zygomycetes." In *The Mycota*, edited by D. J. McLaughlin, E. G. McLaughlin, and P. A. Lemke, 113–146. Berlin Heidelberg: Springer.

Benny, G., R. A. Humber, and K. Voigt. 2014. "Zygomycetous Fungi: Phylum Entomophthoromycota and Subphyla Kickxellomycotina, Mortierellomycotina, Mucoromycotina, and Zoopagomycotina." In *The Mycota VII: Systematics and Evolution Part A*, edited by D. J. McLaughlin and J. W. Spatafora, Second ed., 208–250. Berlin Heidelberg: Springer-Verlag.

Beyens, L., and R. Meisterfeld. 2002. "Protozoa: Testate Amoebae." In *Tracking Environmental Change Using Lake Sediments Vol. 3: Terrestrial, Algal, and Siliceous Indicators*, edited by J. P. Smol, H. J. B. Birks, and W. M. Last, 121–153. New York, Boston, Dordrecht, London, Moscow: Kluwer Academic Publishers.

Braunstein, D. G., and D. R. Lowe. 2001. "Relationship Between Spring and Geyser Activity and the Deposition and Morphology of High Temperature (>73°C) Siliceous Sinter, Yellowstone National Park, Wyoming, U.S.A." *Journal of Sedimentary Research* 71, no. 5: 747–763. https://doi.org/10.1306/2dc40965-0e47-11d7-8643000102c1865d.

Brock, T. D. 1978. *Thermophilic Microorganisms and Life at High Temperatures*, 465. New York: Springer-Verlag. https://doi.org/10.1007/978-1-4612-6284-8.

Brock, T. D. 1994. "Life at High Temperatures." *Science* 230, no. 4722: 132–136. https://doi.org/10.1126/science.230.4722.132.

Browne, P. R. L., and J. V. Lawless. 2001. "Characteristics of Hydrothermal Eruptions, With Examples From New Zealand and Elsewhere." *Earth-Science Reviews* 52, no. 4: 299–331. https://doi.org/10.1016/S0012-8252(00)00030-1.

Burgess, S., P. Statham, J. Holland, and Y.-H. Chou. 2007. "Standardless Quantitative Analysis Using a Drift Detector, What Accuracy is Possible from Live and Reconstructed Data?" *Microscopy and Microanalysis* 13, no. S02. https://doi.org/10.1017/s1431927607072637.

Cady, S. L., and J. D. Farmer. 1996. "Fossilization Processes in Siliceous Thermal Springs: Trends in Preservation Along Thermal Gradients." In *Evolution of Hydrothermal Ecosystems on Earth (And Mars?): Ciba Foundation Symposium*, edited by J. A. Goode, 150–173. Chicester, U.K.: Wiley.

Cady, S. L., J. R. Skok, V. G. Gulick, J. A. Berger, and N. W. Hinman. 2018. "Siliceous Hot Spring Deposits: Why They Remain Key Astrobiological Targets." In *From Habitability to Life on Mars*, edited by N. A. Cabrol and E. A. Grin, 179–210. Amsterdam: Elsevier.

Campbell, K. A., B. Y. Lynne, K. M. Handley, et al. 2015. "Tracing Biosignature Preservation of Geothermally Silicified Microbial Textures

Into the Geological Record." *Astrobiology* 15, no. 10: 858–882. https://doi.org/10.1089/ast.2015.1307.

Campbell, K. A., D. M. Guido, D. A. John, P. G. Vikre, D. Rhys, and A. Hamilton. 2019. "The Miocene Atastra Creek Sinter (Bodie Hills Volcanic Field, California and Nevada): 4D Evolution of a Geomorphically Intact Siliceous Hot Spring Deposit." *Journal of Volcanology and Geothermal Research* 370: 65–81. https://doi.org/10.1016/j.jvolgeores.2018.12.006.

Campbell, K. A., D. M. Guido, P. Gautret, F. Foucher, C. Ramboz, and F. Westall. 2015. "Geyserite in Hot-Spring Siliceous Sinter: Window on Earth's Hottest Terrestrial Paleoenvironment and Its Extreme Life." *Earth-Science Reviews* 148: 44–64. https://doi.org/10.1016/j.earscirev.2015.05.009.

Campbell, K. A., K. Sannazzaro, K. A. Rodgers, N. R. Herdianita, and P. R. L. Browne. 2001. "Sedimentary Facies and Mineralogy of the Late Pleistocene Umukuri Silica Sinter, Taupo Volcanic Zone, New Zealand." *Journal of Sedimentary Research* 71, no. 5: 727–746.

Castenholz, R. W. 1969. "Thermophilic Blue-Green Algae and the Thermal Environment." *Bacteriological Reviews* 33, no. 4: 476–504. https://doi.org/10.1128/br.33.4.476-504.1969.

Channing, A., and D. E. Wujek. 2010. "Preservation of Protists Within Decaying Plants From Geothermally Influenced Wetlands of Yellowstone National Park, Wyoming, United States." *PALAIOS* 25, no. 5: 347–355. https://doi.org/10.2110/palo.2009.p09-057r.

Channing, A., and D. Edwards. 2009. "Silicification of Higher Plants in Geothermally Influenced Wetlands: Yellowstone as a Lower Devonian Rhynie Analog." *PALAIOS* 24, no. 8: 505–521. https://doi.org/10.2110/palo.2008.p08-131r.

Charman, D. J., D. Hendon, W. A. Woodland, and A. Woodland. 2000. *The Identification of Testate Amoebae (Protozoa: Rhizopoda) in Peats*. QRA Technical Guide No 9. London: Quaternary Research Association.

Des Marais, D. J., and M. R. Walter. 2019. "Terrestrial Hot Spring Systems: Introduction." *Astrobiology* 19, no. 12: 1419–1432. https://doi.org/10.1089/ast.2018.1976.

Dick, M. W. 2001. *Straminipilous Fungi*, 668. London: Springer-Science+Business Media, B.V.

Djokic, T., M. J. Van Kranendonk, K. A. Campbell, M. R. Walter, and C. R. Ward. 2017. "Earliest Signs of Life on Land Preserved in ca. 3.5 Ga Hot Spring Deposits." *Nature Communications* 8, no. 1: 1–9. https://doi.org/10.1038/ncomms15263.

Dogiel, V. A. 1965. *General Protozoology*, 747. Oxford: Clarendon Press.

Echeveste, H., R. Fernández, G. Bellieni, et al. 2001. "Relaciones Entre las Formaciones Bajo Pobre y Chon Aike (Jurásico medio a superior) en el área de Estancia El Fénix-Cerro Huemul, Zona Centro-Occidental del Macizo del Deseado, Provincia de Santa Cruz." *Revista de la Asociación Geológica Argentina* 56: 548–558.

Ehrenberg, C. G. 1843. *Verbreitung und Einfluss des mikroskopischen Lebens in Süd- und Nord Amerika*, 183. Berlin: Königliche Akademie der Wissenschaften zu Berlin Physikalische Abhandlungen.

Ellison, R. L., and C. G. Ogden. 1987. "A Guide to the Study and Identification of Fossil Testate Amoebae in Quaternary Lake Sediments." *Internationale Revue der Gesamten Hydrobiologie und Hydrographie* 72, no. 5: 639–652.

Evdokiou, A., F. Marciano-Cabral, and M. Jamerson. 2021. "Studies on the Cyst Stage of *Naegleria fowleri* In Vivo and In Vitro." *Journal of Eukaryotic Microbiology* 69: e12881. https://doi.org/10.1111/jeu.12881.

Farmer, J. 1999. "Taphonomic Modes in Microbial Fossilization." In *Size Limits of Very Small Microorganisms: Proceedings of a Workshop, Space Studies Board, Commission on Physical Sciences, Mathematics and Applications, National Research Council*, edited by A. Knoll, M. J. Osborn, J. Baross, H. C. Berg, N. R. Pace, and M. Sogin, 94–102. Washington, DC: National Academies Press.

Fayers, S. R., and N. H. Trewin. 2003. "A Review of the Palaeoenvironments and Biota of the Windyfield Chert." *Transactions of the Royal Society of Edinburgh: Earth Sciences* 94, no. 4: 325–339. https://doi.org/10.1017/s0263593300000729.

Fernández, L. D., E. Lara, and E. A. D. Mitchell. 2015. "Checklist, Diversity and Distribution of Testate Amoebae in Chile." *European Journal of Protistology* 51, no. 5: 409–424. https://doi.org/10.1016/j.ejop.2015.07.001.

Gangidine, A., M. R. Walter, J. R. Havig, C. Jones, D. M. Sturmer, and A. D. Czaja. 2021. "Trace Element Concentrations Associated With Mid-Paleozoic Microfossils as Biosignatures to aid in the Search for Life." *Lifestyles* 11, no. 2: 142. https://doi.org/10.3390/life11020142.

García Massini, J. L., A. Channing, D. M. Guido, and A. B. Zamuner. 2012. "First Report of Fungi and Fungus-Like Organisms From Mesozoic Hot Springs." *PALAIOS* 27, no. 1: 55–62. https://doi.org/10.2110/palo.2011.p11-076r.

García Massini, J. L., I. H. Escapa, D. M. Guido, and A. Channing. 2016. "First Glimpse of the Silicified Hot Spring Biota From a New Jurassic Chert Deposit in the Deseado Massif, Patagonia, Argentina." *Ameghiniana* 53: 205–230.

González-Miguéns, R., C. Soler-Zamora, M. Villar-Depablo, M. Todorov, and E. Lara. 2022. "Multiple Convergences in the Evolutionary History of the Testate Amoeba Family Arcellidae (Amoebozoa: Arcellinida: Sphaerothecina): When the Ecology Rules the Morphology." *Zoological Journal of the Linnean Society* 94, no. 4: 1044–1071. https://doi.org/10.1093/zoolinnean/zlab074.

Guido, D. M. 2004. "Subdivisión Litofacial e Interpretación del volcanismo jurásico (Grupo Bahía Laura) en el este del Macizo del Deseado, Provincia de Santa Cruz." *Revista de la Asociación Geológica Argentina* 59: 727–742.

Guido, D. M., A. Channing, K. A. Campbell, and A. Zamuner. 2010. "Jurassic Geothermal Landscapes and Fossil Ecosystems at San Agustín, Patagonia, Argentina." *Journal of the Geological Society* 167, no. 1: 11–20. https://doi.org/10.1144/0016-76492009-109.

Guido, D. M., and K. A. Campbell. 2009. "Jurassic Hot-Spring Activity in a Fluvial Setting at La Marciana, Patagonia, Argentina." *Geological Magazine* 146, no. 4: 617–622. https://doi.org/10.1017/s0016756809006426.

Guido, D. M., and K. A. Campbell. 2011. "Jurassic Hot Spring Deposits of the Deseado Massif (Patagonia, Argentina): Characteristics and Controls on Regional Distribution." *Journal of Volcanology and Geothermal Research* 203, no. 1–2: 35–47. https://doi.org/10.1016/j.jvolgeores.2011.04.001.

Guido, D. M., and K. A. Campbell. 2014. "A Large and Complete Jurassic Geothermal Field at Claudia, Deseado Massif, Santa Cruz, Argentina." *Journal of Volcanology and Geothermal* 275: 61–70. https://doi.org/10.1016/j.jvolgeores.2014.02.013.

Guido, D. M., K. A. Campbell, F. Foucher, and F. Westall. 2019. "Life Is Everywhere in Sinters: Examples From Jurassic Hot-Spring Environments of Argentine Patagonia." *Geological Magazine* 156: 1631–1638. https://doi.org/10.1017/S0016756819000815.

Hamilton, A. R., K. A. Campbell, and D. M. Guido. 2019. "Atlas of Siliceous Hot Spring Deposits (Sinter) and Other Silicified Surface Manifestations in Epithermal Environments." Lower Hutt (NZ): GNS Science. 56 p. (GNS Science Report; 2019/06) https://doi.org/10.21420/BQDR-XQ16.

Handley, K. M., K. A. Campbell, B. W. Mountain, and P. R. L. Browne. 2005. "Abiotic-Biotic Controls on the Origin and Development of Specular Sinter: In Situ Growth Experiments, Champagne Pool, Waiotapu, New Zealand." *Geobiology* 3: 93–114.

Handley, K. M., S. J. Turner, K. A. Campbell, and B. W. Mountain. 2008. "Silicifying Biofilm Exopolymers on a Hot-Spring Microstromatolite: Templating Nanometer-Thich Laminae." *Astrobiology* 8: 747–770.

Hedenquist, J. W., and R. W. Henley. 1985. "Hydrothermal Eruptions in the Waiotapu Geothermal System, New Zealand; Their Origin, Associated Breccias, and Relation to Precious Metal Mineralization." *Economic Geology and the Bulletin of the Society of Economic Geologists* 80, no. 6: 1640–1668. https://doi.org/10.2113/gsecongeo.80.6.1640.

Henley, R. W., and A. J. Ellis. 1983. "Geothermal Systems Ancient and Modern: A Geochemical Review." *Earth Science Reviews* 19: 1–50.

Jones, B. 2021. "Siliceous Sinters in Thermal Spring Systems: Review of Their Mineralogy, Diagenesis, and Fabrics." *Sedimentary Geology* 413: 105820. https://doi.org/10.1016/j.sedgeo.2020.105820.

Jones, B., and R. W. Renaut. 1996. "Influence of Thermophilic Bacteria on Calcite and Silica Precipitation in Hot Springs With Water Temperatures Above 90°C: Evidence From Kenya and New Zealand." *Canadian Journal of Earth Sciences* 33, no. 1: 72–83. https://doi.org/10.1139/e96-008.

Jones, B., and R. W. Renaut. 2003. "Petrography and Genesis of Spicular and Columnar Geyserite From the Whakarewarewa and Orakeikorako Geothermal Areas, North Island, New Zealand." *Canadian Journal of Earth Sciences* 40, no. 11: 1585–1610. https://doi.org/10.1139/e03-062.

Jones, B., and R. W. Renaut. 2004. "Water Content of Opal-A: Implications for the Origin of Laminae in Geyserite and Sinter." *Journal of Sedimentary Research* 74, no. 1: 117–128. https://doi.org/10.1306/052403740117.

Jones, B., and R. W. Renaut. 2006. "Growth of Siliceous Spicules in Acidic Hot Springs, Waiotapu Geothermal Area, North Island, New Zealand." *PALAIOS* 21, no. 5: 406–423. https://doi.org/10.2110/palo.2006.p06-026.

Jones, B., and R. W. Renaut. 2011. "Hot Springs and Geysers." In *Encyclopedia of Geobiology*, edited by J. Reitner and V. Thiel, 447–451. Berlin: Springer.

Jones, B., R. W. Renaut, and M. R. Rosen. 1997. "Biogenicity of Silica Precipitation Around Geysers and Hot Spring Vents, North Island, New Zealand." *Journal of Sedimentary Research* 67: 88–104. https://doi.org/10.1306/d42684ff-2b26-11d7-8648000102c1865d.

Jones, B., R. W. Renaut, and M. R. Rosen. 2001. "Taphonomy of Silicified Filamentous Microbes-Implications for Identification." *PALAIOS* 16: 580–592.

Jones, B., R. W. Renaut, and M. R. Rosen. 2003. "Silicified Microbes in a Geyser Mound: The Enigma of Low-Temperature Cyanobacteria in a High-Temperature Setting." *PALAIOS* 18, no. 2: 87–109. https://doi.org/10.1669/0883-1351(2003)18<87:smiagm>2.0.co;2.

Jung, W. 1942. "Südchilenische Thekamöeben." *Archiv für Hydriobiologie* 95: 253–356.

Kerp, H., and B. Bomfleur. 2011. "Photography of Plant Fossils – New Techniques, Old Tricks." *Review of Palaeobotany and Palynology* 166: 117–151.

Knoll, A. H. 1985. "Exceptional Preservation of Photosynthetic Organisms in Silicified Carbonates and Silicified Peats." *Philosophy Transactions of the Royal Society of London, B. Biological Sciences* 311: 111–122. https://doi.org/10.1098/rstb.1985.0143.

Konhauser, K. O., B. Jones, A.-L. Reysenbach, and R. W. Renaut. 2003. "Hot Spring Sinters: Keys to Understanding Earth's Earliest Life Forms." *Canadian Journal of Earth Sciences* 40, no. 11: 1713–1724. https://doi.org/10.1139/e03-059.

Kudryavtsev, A. B., J. W. Schopf, D. G. Agresti, and T. J. Wdowiak. 2001. "In Situ Laser-Raman Imagery of Precambrian Microscopic Fossils." *Proceedings of the National Academy of Sciences of the United States of America* 98, no. 3: 823–826. https://doi.org/10.1073/pnas.98.3.823.

Lahr, D., and S. Lopes. 2009. "Evaluating the Taxonomic Identity in Four Species of the Lobose Testate Amoebae Genus *Arcella* Ehrenberg, 1832." *Acta Protozoologica* 48: 127–142.

Lamentowicz, M., K. Kajukało-Drygalska, P. Kołaczek, V. E. J. Jassey, M. Gąbka, and M. Karpińska-Kołaczek. 2020. "Testate Amoebae Taxonomy and Trait Diversity Are Coupled Along an Openness and Wetness Gradient in Pine-Dominated Baltic Bogs." *European Journal of Protistology* 73: 125674. https://doi.org/10.1016/j.ejop.2020.125674.

Lowe, D. R., and D. Braunstein. 2003. "Microstructure of High-Temperature (>73°C) Siliceous Sinter Deposited Around Hot Springs and Geysers, Yellowstone National Park: The Role of Biological and Abiological Processes in Sedimentation." *Canadian Journal of Earth Sciences* 40: 1611–1642. https://doi.org/10.1139/e03-066.

Lowe, D. R., K. S. Anderson, and D. Braunstein. 2001. "The Zonation and Structuring of Siliceous Sinter Around Hot Springs, Yellowstone National Park, and the Role of Thermophilic Bacteria in Its Deposition." In *Thermophiles: Biodiversity, Ecology and Evolution*, edited by A. M. Reysenbach, M. Voytech, and R. Mancinelli, 143–166. New York: Kluwer Academic/Plenum Publishers.

Lynne, B. Y. 2012. "Mapping Vent to Distal-Apron Hot Spring Paleo-Flow Pathways Using Siliceous Sinter Architecture." *Geothermics* 43: 3–24. https://doi.org/10.1016/j.geothermics.2012.01.004.

Lynne, B. Y., K. A. Campbell, B. J. James, P. R. L. Browne, and J. Moore. 2007. "Tracking Crystallinity in Siliceous Hot-Spring Deposits." *American Journal of Science* 307: 612–641. https://doi.org/10.2475/03.2007.03.

Maliva, R. G., A. H. Knoll, and B. M. Simonson. 2005. "Secular Change in the Precambrian Silica Cycle: Insights From Chert Petrology." *GSA Bulletin* 117: 835–845. https://doi.org/10.1130/b25555.1.

Marchionni, D. S., R. E. De Barrio, M. O. Tessone, M. A. Del Blanco, and H. J. Echeveste. 1999. "Hallazgo de Estructuras Estromatolíticas Jurásicas en el Macizo del Deseado, Provincial de Santa Cruz." *Revista de la Asociación Geológica Argentina* 54: 173–176.

Marcisz, K., V. E. Jassey, A. Kosakyan, et al. 2020. "Testate Amoeba Functional Traits and Their Use in Paleoecology." *Frontiers in Ecology and Evolution* 8: 5966. https://doi.org/10.3389/fevo.2020.575966.

Marshall, A. O., R. L. Wehrbein, B. S. Lieberman, and C. P. Marshall. 2012. "Raman Spectroscopic Investigations of Burgess Shale-Type Preservation: A New Way Forward." *PALAIOS* 27, no. 5: 288–292. https://doi.org/10.2110/palo.2011.p11-041r.

Mazei, Y., and A. Tsyganov. 2006. *Freshwater Testate Amoebae*, 300. Moscow: KMK Sci Press.

McKeown, M. M., J. M. Wilmshurst, C. Duckert, J. R. Wood, and E. A. D. Mitchell. 2019. "Assessing the Ecological Value of Small Testate Amoebae (<45 μm) in New Zealand Peatlands." *European Journal of Protistology* 68: 1–16.

Meyer-Dombard, D. R., E. L. Schock, and J. P. Amend. 2005. "Archaeal and Bacterial Communities in Geochemically Diverse Hot Springs of Yellowstone National Park, USA." *Geobiology* 3, no. 3: 211–227. https://doi.org/10.1111/j.1472-4669.2005.00052.x.

Meyer-Dombard, D. R., W. Swingley, J. Raymond, J. Havig, E. L. Schock, and R. E. Summons. 2011. "Hydrothermal Ecotones and Streamer Biofilm Communities in the Lower Geyser Basin, Yellowstone National Park." *Environmental Microbiology* 13, no. 8: 2216–2231. https://doi.org/10.1111/j.1462-2920.2011.02476.x.

Munoz-Saez, C., J. Gong, A. Perez-Fodich, and M. A. van Zuilen. 2023. "Environmental and Hydrogeochemical Controls of Spicular Geyserite in Opaline Hot Spring Deposits." *Earth and Space Science* 10, no. 3: e2022EA002645. https://doi.org/10.1029/2022ea002645.

Murphy, R. J., M. J. Van Kranendonk, R. Baumgartner, and C. Ryan. 2021. "Biogenicity of Spicular Geyserite From Te Kopia, New Zealand: Integrated Petrography, High-Resolution Hyperspectral and Elemental Analysis." *Astrobiology* 21, no. 1: 115–135. https://doi.org/10.1089/ast.2019.2067.

Nersezova, E. E., M. C. Rowe, K. A. Campbell, et al. 2024. "In Review. Trace Metal and Organic Biosignatures in Digitate Stromatolites From Terrestrial Siliceous Hot Spring Deposits: Implications for Mars Life Exploration." *Chemical Geology* 661: 122194.

Ogden, C. G., and R. H. Hedley. 1980. "An Atlas of Freshwater Testate Amoebae." *Soil Science* 130, no. 3: 176. https://doi.org/10.1097/00010694-198009000-00013.

Pankhurst, R. J., T. R. Riley, C. M. Fanning, and S. P. Kelley. 2000. "Episodic Silicic Volcanism in Patagonia and the Antarctic Peninsula: Chronology of Magmatism Associated With the Break-Up of Gondwana." *Journal of Petrology* 45, no. 5: 605–625. https://doi.org/10.1093/petrology/41.5.605.

Petryshyn, V. A., E. N. Junkins, B. W. Stamps, et al. 2021. "Builders, Tenants, and Squatters: The Origins of Genetic Material in Modern Stromatolites." *Geobiology* 19, no. 3: 261–277. https://doi.org/10.1111/gbi.12429.

Piper, J. 2010. "Software-Based Stacking Techniques to Enhance Depth of Field and Dynamic Range in Digital Photomicrography." *Methods in Molecular Biology* 611: 193–210. https://doi.org/10.1007/978-1-60327-345-9_16.

Powell, M. J. 1993. "Looking at Mycology With a Janus Face: A Glimpse at Chytridiomycetes Active in the Environment." *Mycologia* 85, no. 1: 1–20. https://doi.org/10.1080/00275514.1993.12026239.

Powell, M. J., and P. M. Letcher. 2014. "Chytridiomycota, Monoblepharidomycota and Neocallimastigomycota." In *The Mycota VIIA*, edited by D. J. McLaughlin and J. W. Spatafora, 141–176. Austria: Springer-Verlag.

Renaut, R. W., and B. Jones. 2000. "Microbial Precipitates Around Continental Hot Springs and Geysers." In *Microbial Sediments*, edited by R. E. Riding and S. M. Awramik, 187–195. Berlin: Springer.

Richardson, N. J., and J. R. Underhill. 2002. "Controls on the Structural Architecture and Sedimentary Character of Syn-Rift Sequences, North Falkland Basin, South Atlantic." *Marine and Petroleum Geology* 19: 417–443. https://doi.org/10.1016/s0264-8172(02)00024-7.

Riley, T. R., P. T. Leat, R. J. Pankhurst, and C. Harris. 2001. "Origins of Large Volume Rhyolitic Volcanism in the Antarctic Peninsula and Patagonia by Crustal Melting." *Journal of Petrology* 42, no. 6: 1043–1065. https://doi.org/10.1093/petrology/42.6.1043.

Ruiz González, V., E. M. Renda, H. Vizán, M. Ganerød, C. G. Puigdomenech, and C. B. Zaffarana. 2022. "Deformation Along the Deseado Massif (Patagonia, Argentina) During the Jurassic Period and Its Relationship With the Gondwana Breakup: Paleomagnetic and Geochronological Constraints." *Tectonophysics* 834: 229389. https://doi.org/10.1016/j.tecto.2022.229389.

Sagasti, A. J., J. L. García Massini, I. H. Escapa, and D. M. Guido. 2019. "Multitrophic Interactions in a Geothermal Setting: Arthropod Borings, Actinomycetes, Fungi and Fungal-Like Microorganisms in a Decomposing Conifer Wood From the Jurassic of Patagonia." *Palaeogeography, Palaeoclimatology, Palaeoecology* 5141: 31–44. https://doi.org/10.1016/j.palaeo.2018.09.004.

Saitoh, M., N. Olivier, M. Garçon, et al. 2021. "Metamorphic origin of anastomosing and wavy laminas overprinting putative microbial deposits from the 3.22 Ga Moodies Group (Barberton Greenstone Belt)." *Precambrian Research* 362: 106306. https://doi.org/10.1016/j.precamres.2021.106306.

Schalamuk, I., M. Zubia, A. Gennini, and R. R. Fernandez. 1997. "Jurassic Epithermal Au–Ag Deposits of Patagonia, Argentina." *Ore Geology Reviews* 12: 173–186.

Schopf, J. W., A. B. Kudryavtsev, D. G. Agresti, A. D. Czaja, and T. J. Wdowiak. 2005. "Raman Imagery: A New Approach to Assess the Geochemical Maturity and Biogenicity of Permineralized Precambrian Fossils." *Astrobiology* 5, no. 3: 333–371. https://doi.org/10.1089/ast.2005.5.333.

Schopf, J. W., and A. B. Kudryavtsev. 2009. "Confocal Laser Scanning Microscopy and Raman Imagery of Ancient Microscopic Fossils." *Precambrian Research* 173, no. 1–4: 39–49. https://doi.org/10.1016/j.precamres.2009.02.007.

Schulz, G., M. Maraun, E. Völcker, S. Scheu, and V. Krashevska. 2018. "Evaluation of Morphological Characteristics to Delineate Taxa of the Genus *Trigonopyxis* (Amoebozoa, Arcellinida)." *Protist* 169: 190–205. https://doi.org/10.1016/j.protis.2018.02.005.

Siemensma, F. 2023. "Lobose Testate Amoebae." https://arcella.nl/lobose-testate-amoebae/.

Sillitoe, R. H. 2015. "Epithermal Paleosurfaces." *Mineralium Deposita* 50: 767–793. https://doi.org/10.1007/s00126-015-0614-z.

Šímová, A., M. Jiroušek, P. Singh, P. Hájková, and M. Hájek. 2022. "Ecology of Testate Amoebae Along an Environmental Gradient From Bog to Calcareous Fens in East-Central Europe: Development of Transfer Functions for Palaeoenvironmental Reconstructions." *Palaeogeography, Palaeoclimatology, Palaeoecology* 601: 111145. https://doi.org/10.1016/j.palaeo.2022.111145.

Slagter, S., W. Hao, N. J. Planavsky, K. O. Konhauser, and L. G. Tarhan. 2022. "Biofilms as Agents of Ediacara-Style Fossilization." *Scientific Reports* 12: 8631. https://doi.org/10.1038/s41598-022-12473-1.

Sriaporn, C., K. A. Campbell, M. Millan, S. W. Ruff, M. J. Van Kranendonk, and K. M. Handley. 2020. "Stromatolitic Digitate Sinters Form Under Wide-Ranging Physicochemical Conditions With Diverse Hot Spring Microbial Communities." *Geobiology* 18, no. 5: 619–640.

Strullu-Derrien, C., P. Kenrick, T. Goral, and A. H. Knoll. 2019. "Testate Amoebae in the 407 Million-Year-Old Rhynie Chert." *Current Biology* 29, no. 3: 461–467. https://doi.org/10.1016/j.cub.2018.12.009.

Strullu-Derrien, C., T. Goral, J. E. Longcore, J. Olesen, P. Kenrick, and G. D. Edgecombe. 2016. "A New Chytridiomycete Fungus Intermixed With Crustacean Resting Eggs in a 407-Million-Year-Old Continental Freshwater Environment." *PLoS One* 11: e0167301. https://doi.org/10.1371/journal.pone.0167301.

Strullu-Derrien, C., Z. Wawrzyniak, T. Goral, and P. Kenrick. 2015. "Fungal Colonization of the Rooting System of the Early Land Plant *Asteroxylon mackiei* From the 407-Myr-Old Rhynie Chert (Scotland, UK)." *Botanical Journal of the Linnean Society* 179: 201–213.

Teece, B. L., D. M. Guido, K. A. Campbell, M. J. Van Kranendonk, A. Galar, and S. C. George. 2022. "Exceptional Molecular Preservation in the Late Jurassic Claudia Palaeo-Geothermal Field (Deseado Massif, Patagonia, Argentina)." *Organic Geochemistry* 173: 104504. https://doi.org/10.1016/j.orggeochem.2022.104504.

Trewin, N. H. 1993. "Depositional Environment and Preservation of Biota in the Lower Devonian Hot-Springs of Aberdeenshire, Scotland." *Earth and Environmental Science Transactions of the Royal Society of Edinburgh* 84, no. 3–4: 433–442. https://doi.org/10.1017/s0263593300006234.

Tsyganov, A. N., K. V. Babeshko, and Y. A. Mazei. 2016. *A Guide to Testate Amoebae With the Keys to Genera*, 132. Penza: PSU Publishing House: Russian Science Foundation.

Van Kranendonk, M. J., K. Campbell, E. Barlow, et al. 2019. "A Pyramid of Life Detection for Ancient Life, Based on Deep-Time Earth Experience." *Astrobiology Science Conference (AbSciCon)* 2019: 342–355.

Walter, M. R. 1976. "Hot-Spring Sediments in Yellowstone National Park." In *Stromatolites*, edited by M. R. Walter, 489–498. Amsterdam: Elsevier.

Walter, M. R., J. P. Grotzinger, and J. W. Schopf. 1992. "Proterozoic stromatolites." In *The Proterozoic Biosphere: A Multidisciplinary Study*,

edited by J. W. Schopf and C. Klein, 253–260. Cambridge: Cambridge University Press.

Watkinson, S. C., L. Boddy, and N. P. Money. 2016. *The Fungi*. 3rd ed, 453. UK: Elsevier-Academic Press.

Webb, G. E., and B. S. Kamber. 2011. "Trace Element Geochemistry as a Tool for Interpreting Microbialites." In *Earliest Life on Earth: Habitats, Environments and Methods of Detection*, 127–170. Netherlands: Springer.

Westall, F., K. A. Campbell, J.-G. Brérhéret, et al. 2015. "Archean (3.33 Ga) Microbe-Sediment Systems Were Diverse and Flourished in a Hydrothermal Context." *Geology* 43: 615–618. https://doi.org/10.1130/g36646.1.

Westall, F., K. Hickman-Lewis, N. Hinman, et al. 2018. "A Hydrothermal-Sedimentary Context for the Origin of Life." *Astrobiology* 18, no. 3: 259–293. https://doi.org/10.1089/ast.2017.1680.

Winterbourn, M. J., and T. J. Brown. 1967. "Observations on the Faunas of Two Warm Streams in the Taupo Thermal Region." *New Zealand Journal of Marine and Freshwater Research* 1, no. 1: 38–50. https://doi.org/10.1080/00288330.1967.9515190.

Zhang, Y., G. Wu, H. Jiang, et al. 2018. "Abundant and Rare Microbial Biospheres Respond Differently to Environmental and Spatial Factors in Tibetan Hot Springs." *Frontiers in Microbiology* 9: 2093. https://doi.org/10.3389/fmicb.2018.02096.

Supporting Information

Additional supporting information can be found online in the Supporting Information section.